

Methoden moderner Röntgenphysik II: Streuung und Abbildung

Vorlesung zum Haupt- oder Masterstudiengang Physik, SoSe 2019

G. Grübel, F. Lehmkühler, L. Müller, O. Seeck

Location Lecture hall INF, Physics, Jungiusstraße 11

Time Tuesday 12:30 - 14:30
 Thursday 8:30 - 10:00

Outline

Part II/1:

Studies on Magnetic Nanostructures

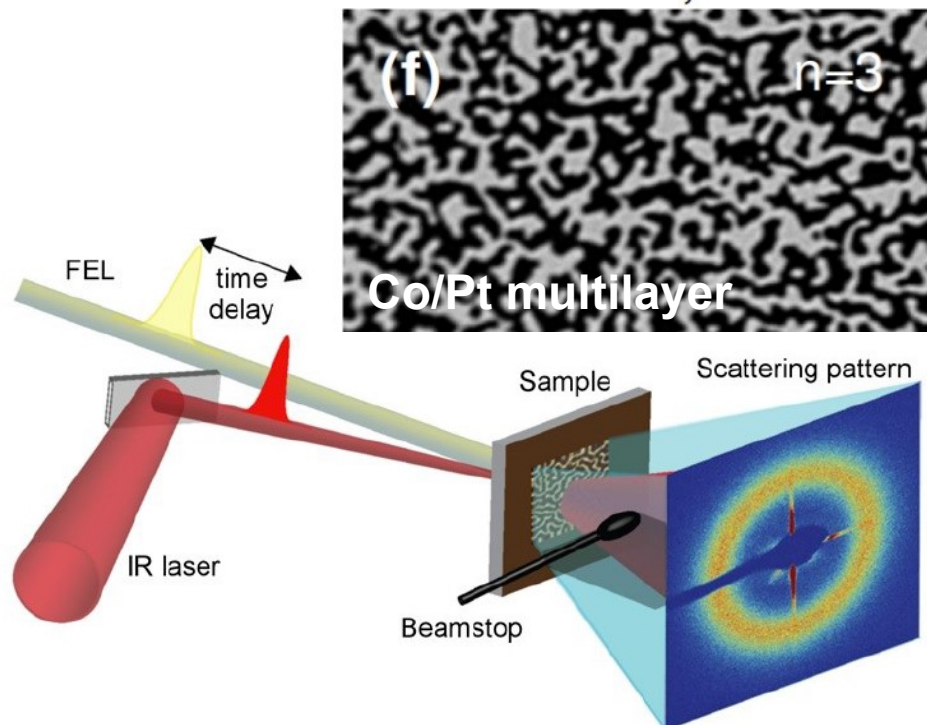
by Leonard Müller

[28.5.] Ferromagnetism in a Nutshell

- Introduction to Magnetic Materials
- Magnetic Phenomena
- Magnetic Free Energy
- Perpendicular Magnetic Anisotropy
- Magnetic Domains and Domain Walls

[4.6.] Interaction of Polarized Photons with Ferromagnetic Materials

- Charge and Spin X-ray Scattering by a Single Electron
- Absorption and Resonant Scattering of Ferromagnets
(Semi-Classical and Quantum-Mechanical Concepts)



B. Pfeu et al., *Nature Communications*, Vol. 3, 11; DOI:doi:10.1038/ncomms2108 (2012)
L. Müller et al., *Rev. Sci. Instrum.* 84, 013906 (2013)

Outline

Part II/2:

Studies on Magnetic Nanostructures

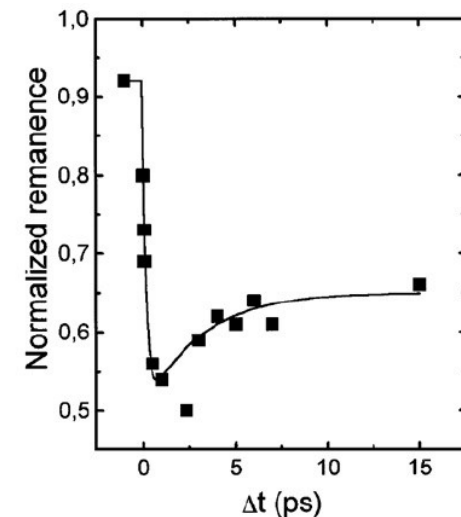
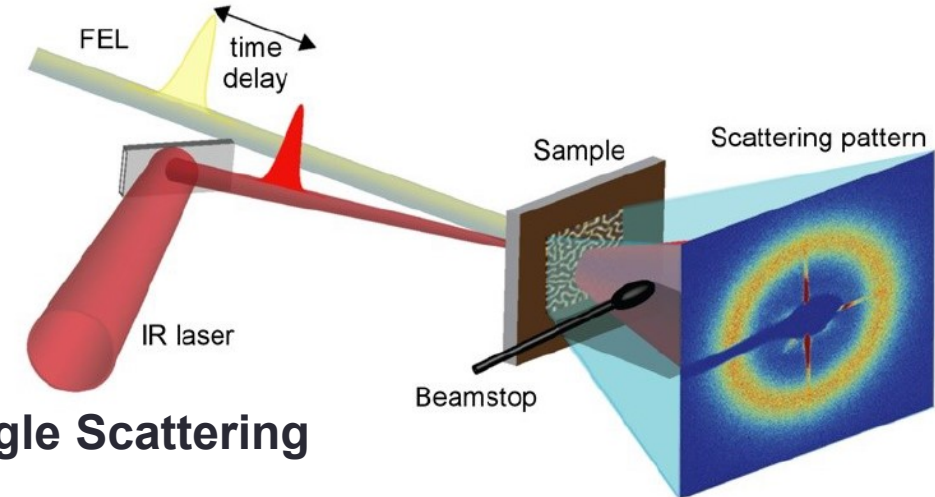
by Leonard Müller

[6.6.] X-ray Magnetic Circular Dichroism (XMCD) & Resonant Magnetic Small-Angle Scattering (mSAXS)

- Role of Spin-Orbit Coupling and Exchange Splitting
- Sum Rules
- XMLD and Natural Dichroism
- mSAXS of Magnetic Domain Patterns

[18.6.] Femtomagnetism

- Introduction to Ultrafast Magnetization Dynamics Induced by Femtosecond Infrared Pulses
- Pump-Probe Experiments of Nano-Scale Magnetic Domain Patterns
- All-Optical Switching
- Manipulating Magnetism by XUV and THz Pulses



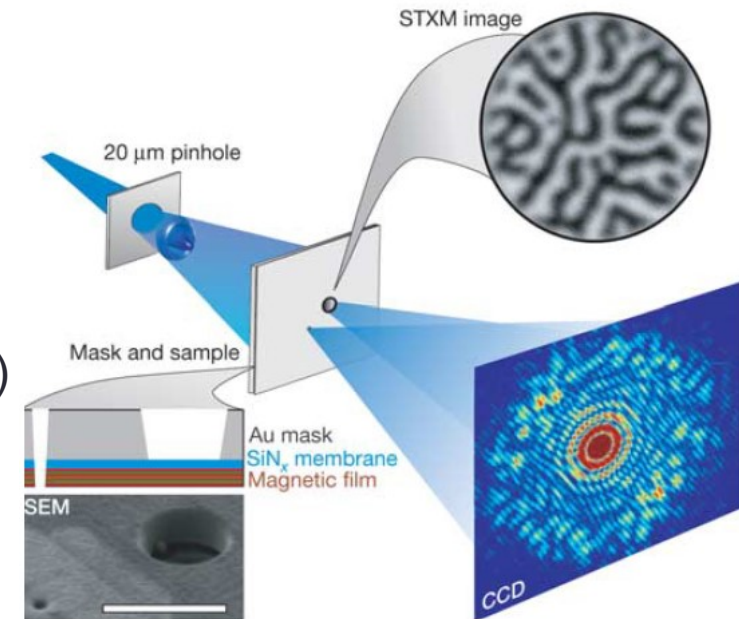
Part II/3:

Studies on Magnetic Nanostructures

by Leonard Müller

[20.6.] Imaging of Magnetic Domains

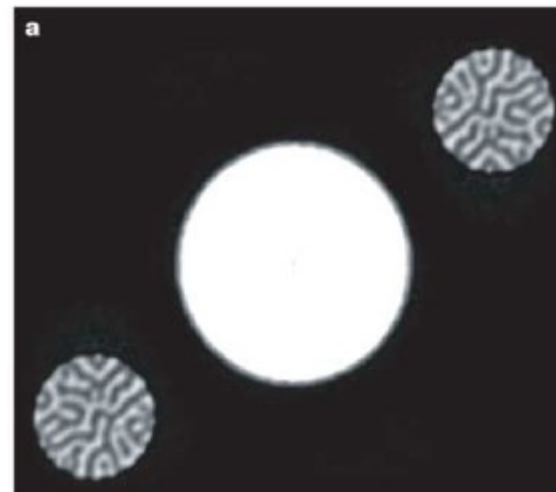
- **Fourier Transform Holography (FTH)**
- Scanning Transmission X-ray Microscopy (STXM)
- Coherent Diffraction Imaging (CDI)



Lensless imaging of magnetic nanostructures by X-ray spectro-holography

S. Eisebitt¹, J. Lüning², W. F. Schlotter^{2,3}, M. Lörgen¹, O. Hellwig^{1,4},
W. Eberhardt¹ & J. Stöhr²

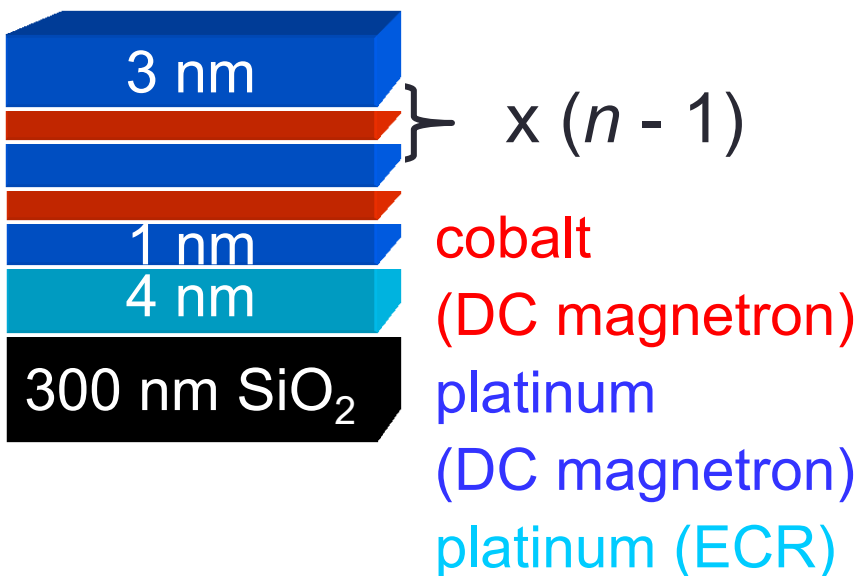
NATURE | VOL 432 | 16 DECEMBER 2004 |



Co/Pt Multilayers

Layer Composition

Multilayer stack ($n = 1 - 32$)



Perpendicular magnetic anisotropy in Co/Pt discovered in 1988

Garcia et al., J. Appl. Phys. **63**, 5066 (1988)

Magnetic Domains

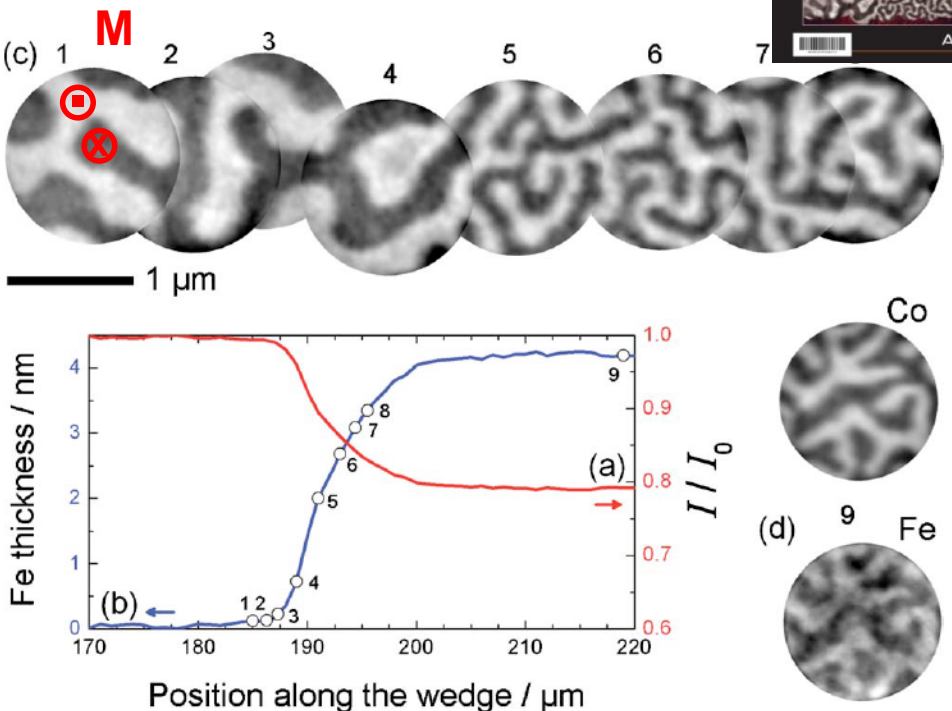


FIG. 3. (Color online) Domain size evolution of a Co/Pt multilayer film covered by an iron wedge. Plot (a) gives the absorption profile (normalized photodiode current) at the Fe L_3 absorption edge when scanning over the Fe wedge. The absorption is used to calculate the local iron overlayer thickness (b). A contiguous series of XMCD holograms at the Co L_3 absorption edge has been acquired and reconstructed (c) at the indexed positions along the iron wedge. Image (d) has been measured at the Fe L_3 absorption edge at the very same position as the last Co image (#9).

D. Stickler, G. Grübel, H. P. Oepen et al., Appl. Phys. Lett. **96**, 042501 (2010)

Co/Pt Multilayers

Structural analysis

X-ray diffraction (XRD) to determine crystallinity

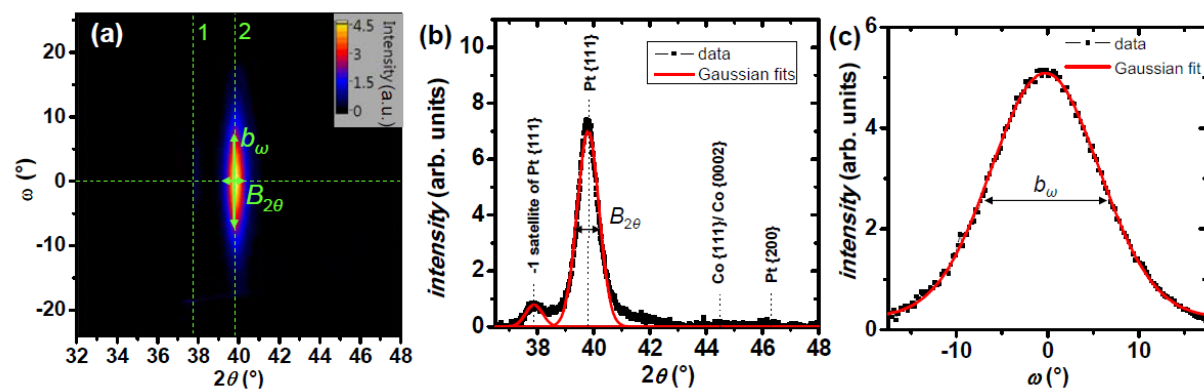
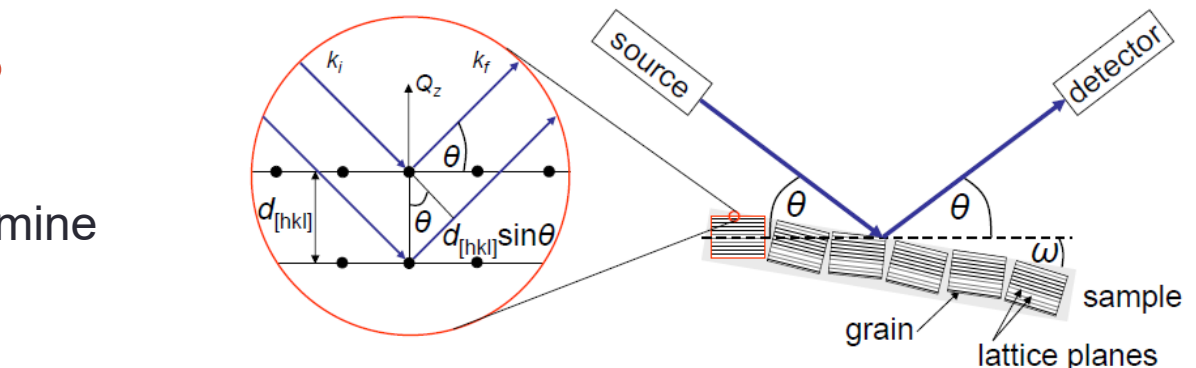
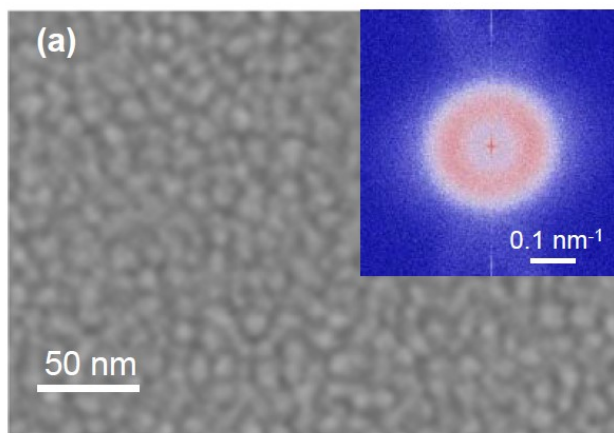


Figure 5.17: (a) Diffraction map $I(\omega, 2\theta)$ of a 5 nm Pt / (0.8 nm Co / 4 nm Pt)₃ / 0.8 nm Co / 3 nm Pt multilayer grown on Si₃N₄. The intensity is color coded according to the given color bar. The positions of the -1 satellite reflex (1) and of the peak at the Pt(111) position (2) are indicated by vertical dashed lines. (b) shows the integrated intensity $I(2\theta) = \sum_\omega I(\omega, 2\theta)$ and (c) the cross-section $I(\omega)$ at the peak position $2\theta_{\text{fcc Pt}(111)} = 39.8^\circ$. Both curves are fitted to a normal distribution (red lines) with a FWHM of $B_{2\theta}$ and b_ω , respectively.

- Co and Pt layers have fcc lattice
- polycrystalline,
- grain size of (11 ± 2) nm
- out-of-plane textured,
- tilting of grains (FWHM): $(23 \pm 2)^\circ$

More details, see G. Winkler, A. Kobs, A. Chuvilin, D. Lott, A. Schreyer, H. P. Oepen, J. Appl. Phys. **117**, 105306 (2015)

Co/Pt Multilayers

Structural analysis

X-ray reflectometry (XRR) to determine quality of layered structure

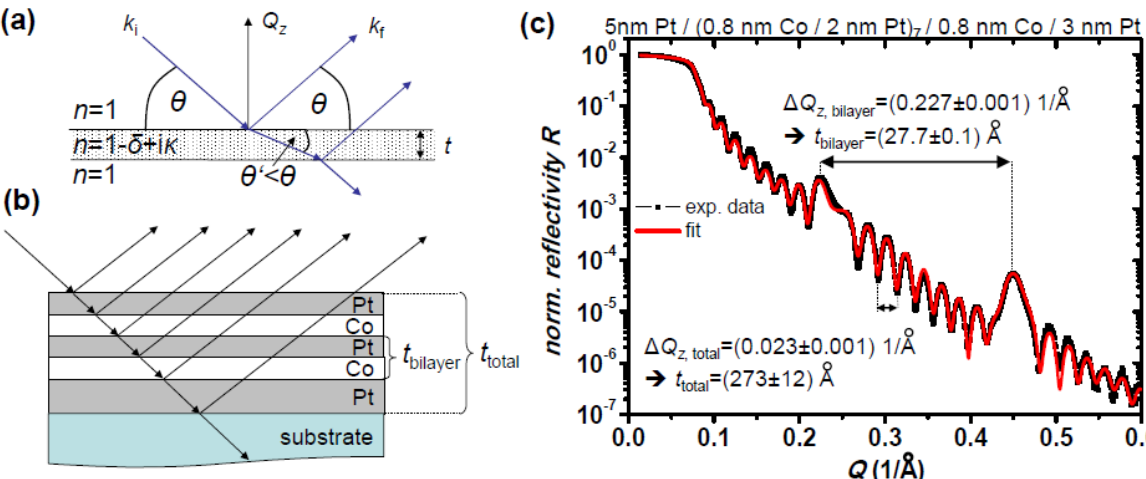


Figure 5.27: (a) Refraction and reflection of an x-ray beam hitting a thin layer with thickness t . The interference of the partial waves refracted from the two interfaces generates oscillations (Kiessig fringes) in the reflectivity profile $R(\theta)$. (b) In a periodically layered structure the interferences of the reflected partial waves additionally yield beating waves in $R(\theta)$. (c) Reflectivity R in dependence of the scattering vector Q_z for a multilayer with $n = 8$ and a Pt interlayer thickness of $t_{\text{Pt}} = 2 \text{ nm}$. From the oscillation and beating wave period the total thickness of the stacking and the bilayer thickness was verified utilizing Eq. 5.64 and Eq. 5.65, respectively. The red solid line is a fit utilizing the software PAR-RAT32 [715], which is used in particular to determine the thickness of the roughness/interdiffusion regions.

A. Kobs, PhD thesis, Universität Hamburg (2013)

$$\Delta Q_z, \text{total} = \frac{2\pi}{t_{\text{total}}}$$

$$\Delta Q_z, \text{bilayer} = \frac{2\pi}{t_{\text{bilayer}}}$$

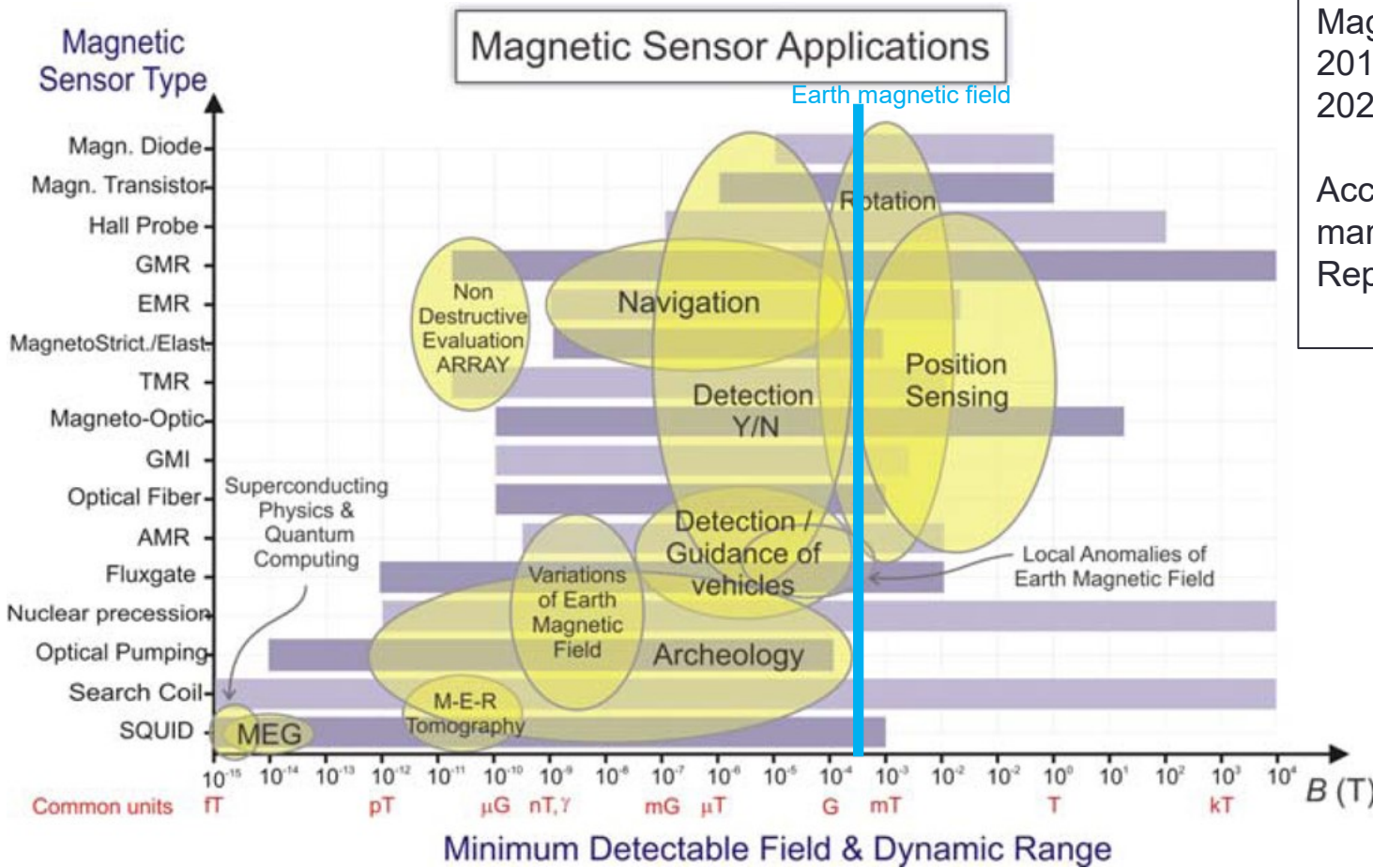
- roughness: $(0.2 \pm 0.1) \text{ nm}$
- interdiffusion of Co & Pt: $(0.5 \pm 0.2) \text{ nm}$

disentangling of both from off-specular scans



Introduction to Magnetic Materials

Magnetic Materials in Sensor Applications



Magnetic Sensor Market:
 2016: USD 2.96 Billion
 2023: USD 5.37 Billion

Acc. to
marketsandmarkets.com,
 Report Code: SE 2688

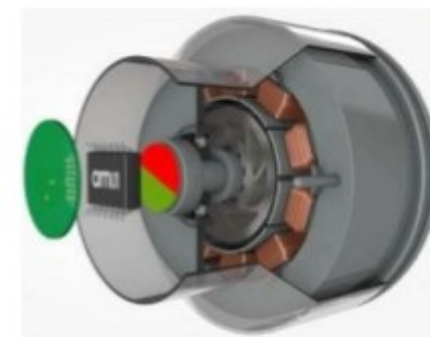
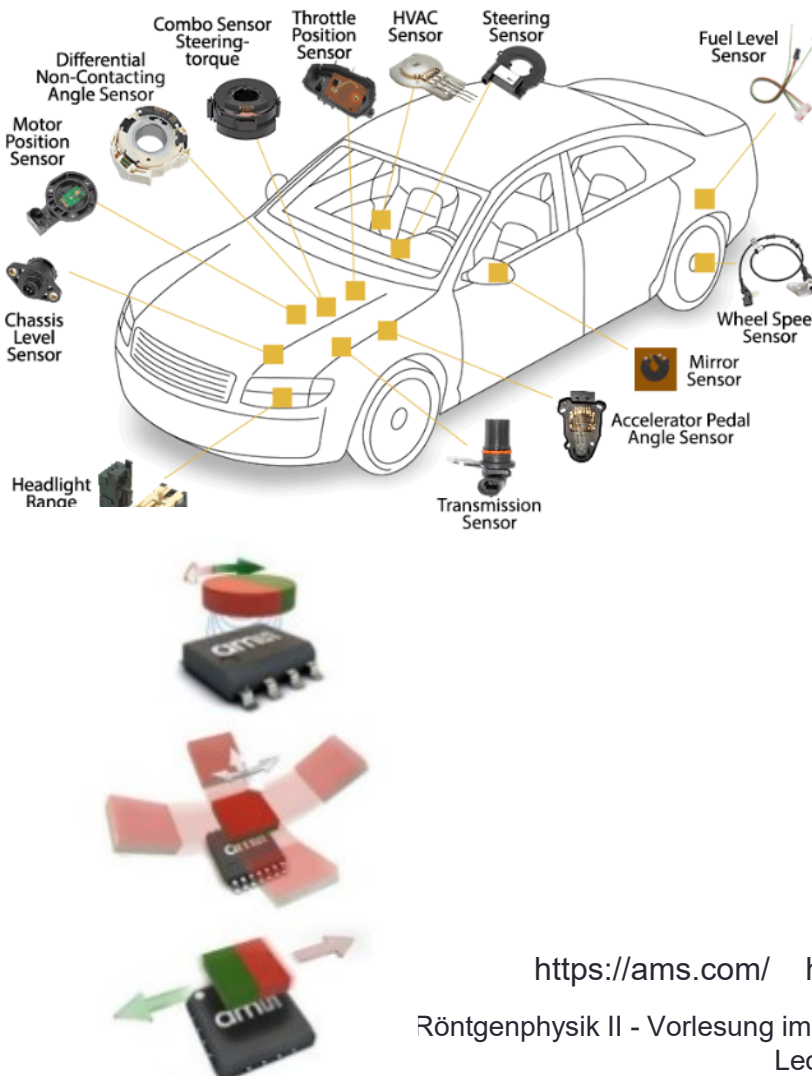
M. Díaz-Michelena, Sensors 9, 2271 (2009)

Methoden Moderner Röntgenphysik II - Vorlesung im Haupt-/Masterstudiengang, Universität Hamburg, SoSe 2019,
 Leonard Müller



Introduction to Magnetic Materials

Magnetic Materials in Sensor Applications



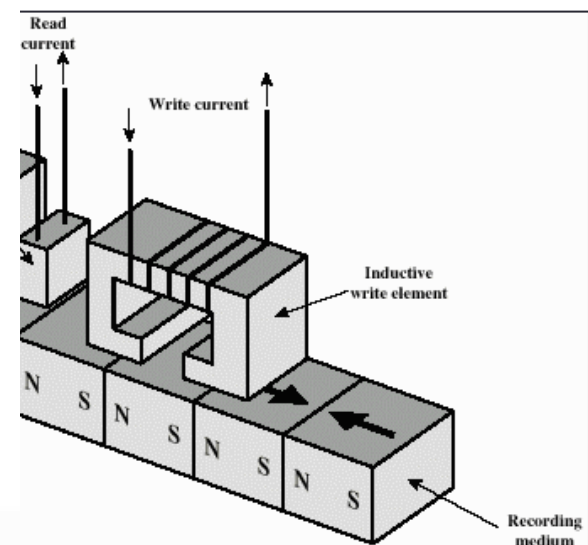
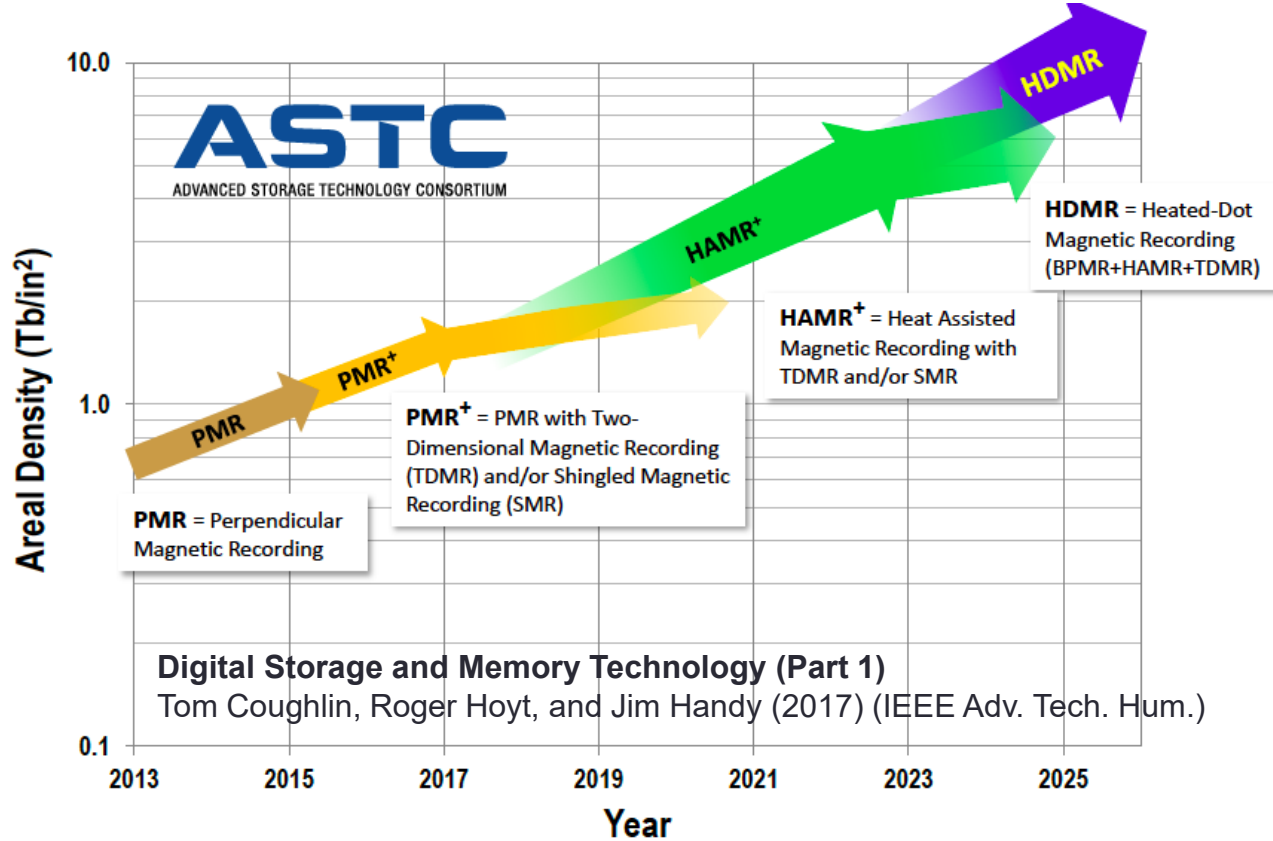
<https://ams.com/> <http://www.vectormagnets.com>

Röntgenphysik II - Vorlesung im Haupt-/Masterstudiengang, Universität Hamburg, SoSe 2019,
Leonard Müller



Introduction to Magnetic Materials

Temporal Evolution of Storage Density in HDD

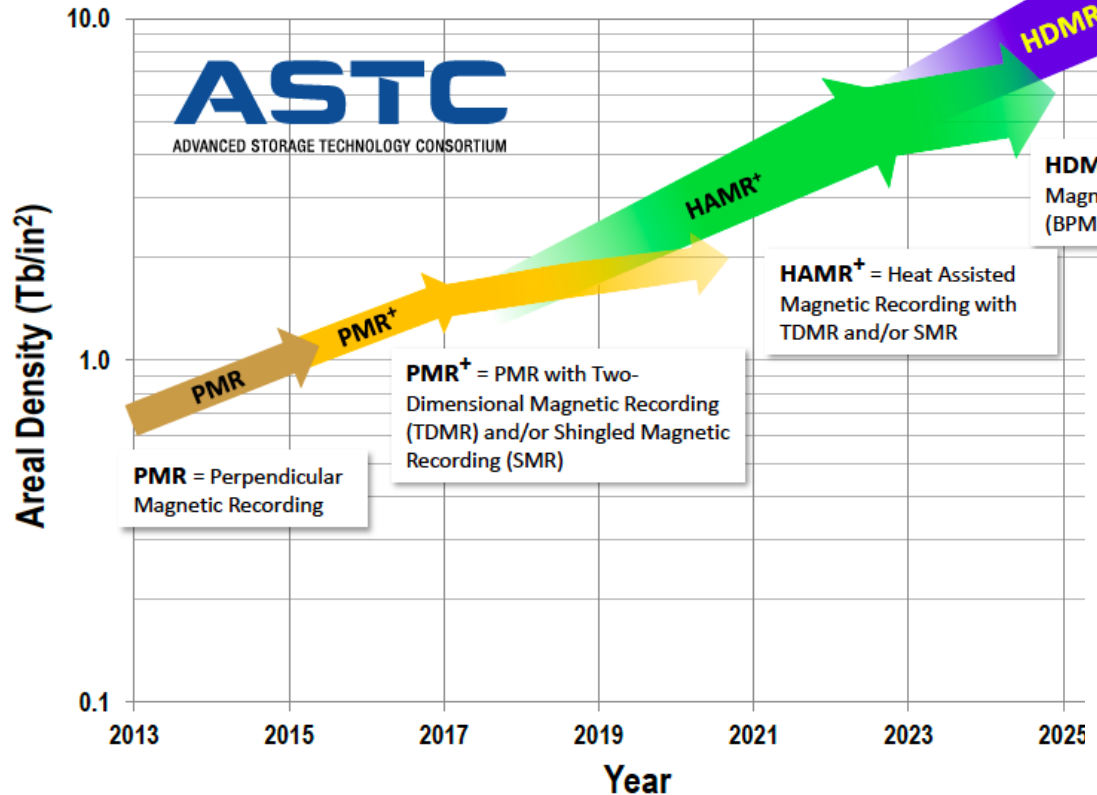


IDEMA®

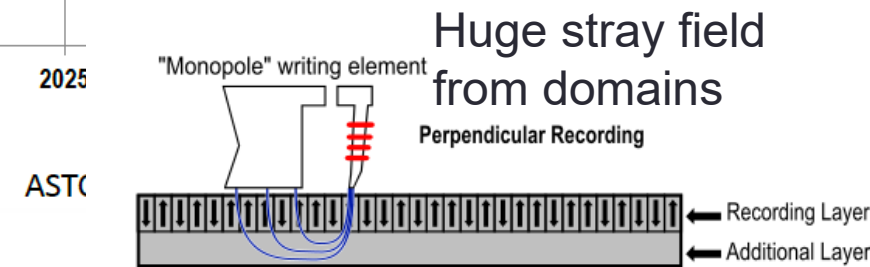
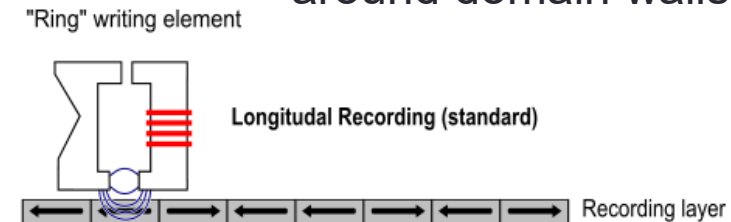
ASTC Proprietary

Introduction to Magnetic Materials

Temporal Evolution of Storage Density in HDD



Low stray field around domain walls

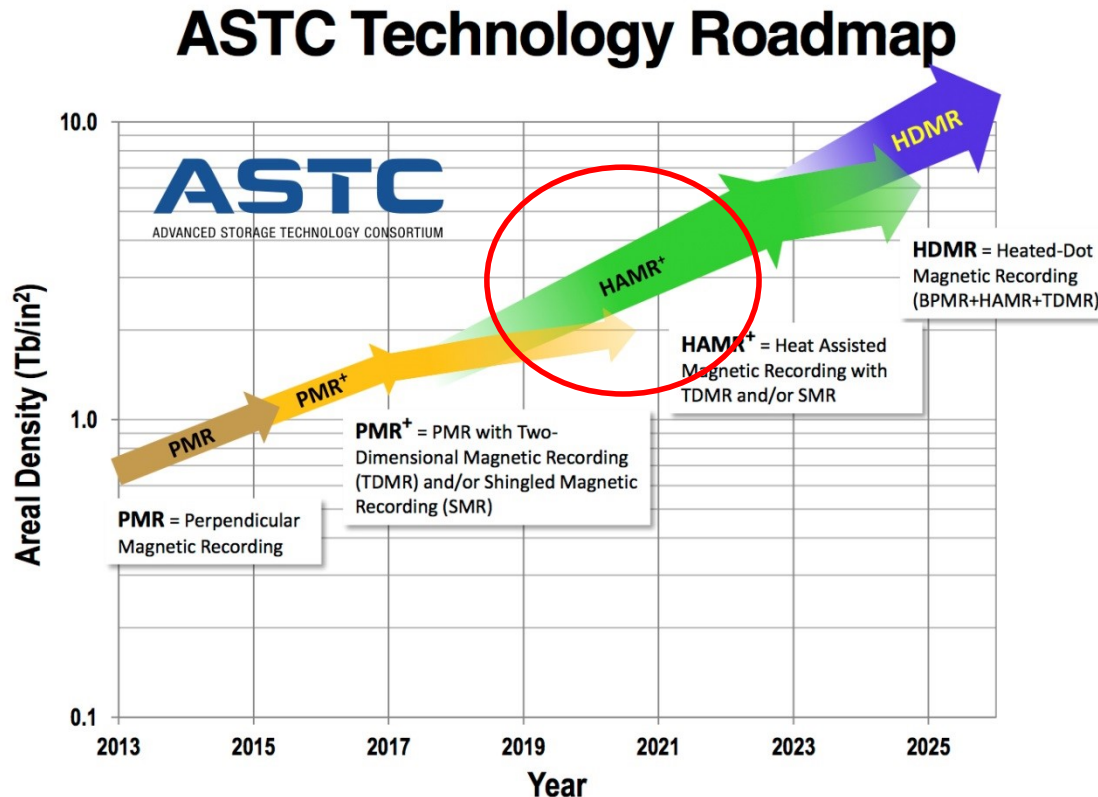


IDEMA

ASTC

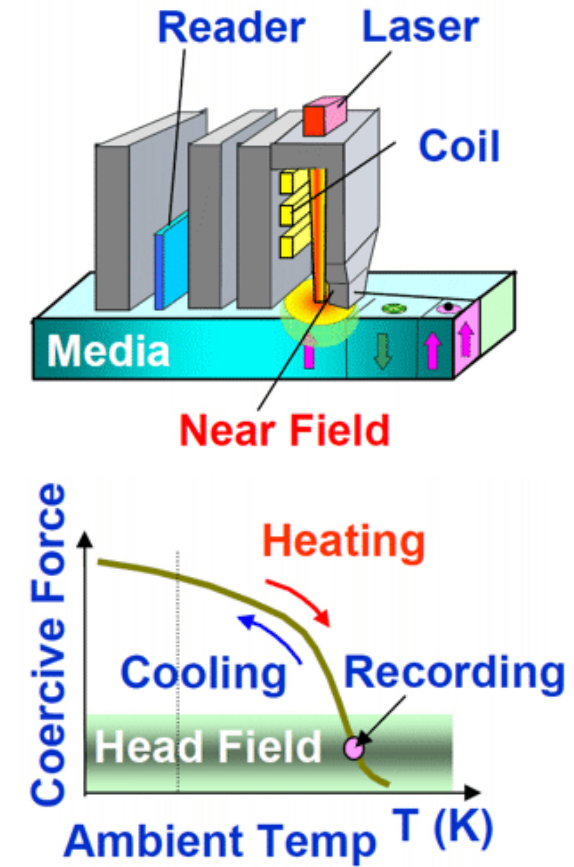
Introduction to Magnetic Materials

Temporal Evolution of Storage Density in HDD



IDEMA®

ASTC Confidential



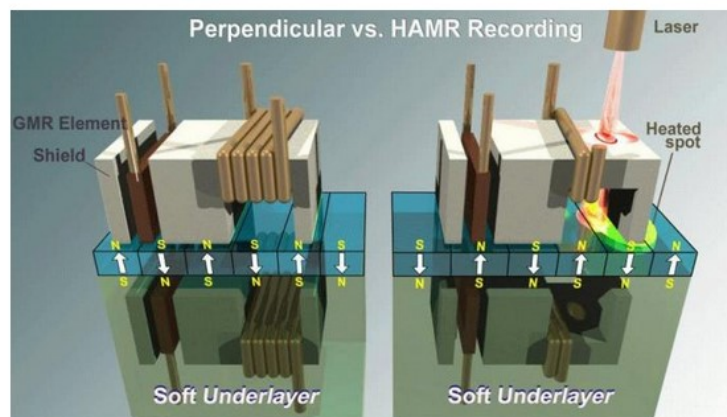
Introduction to Magnetic Materials

Temporal Evolution of Storage Density in HDD

Seagate: HAMR-Festplatten Ende 2018, 20-TByte-Laufwerke ein Jahr später

24.10.2017 17:40 Uhr – Lutz Labs

vorlesen



Seagate bleibt dem einmal eingeschlagenen Weg treu: 2018 will das Unternehmen Festplatten mit HAMR-Technik auf den Markt bringen.

Das wird spannend: Western Digital setzt auf MAMR, Seagate [weiter auf HAMR](#). Ob sich eine der beiden Techniken zur Erhöhung der Festplattenkapazität durchsetzen wird, bleibt sicher noch einige Zeit unklar. Anders als bei den ebenfalls kapazitätssteigernden Techniken Helium-Füllung und Shingled Magnetic Recording sind aber nun erstmals zwei Unternehmen mit konkurrierender Technik auf dem Vormarsch.

Seagate-Chef Dr. Mark Re wirbt im [Seagate-Blog](#) für die HAMR-Technik. Mit HAMR, Heat Assisted Magnetic Recording, seien bereits heute Kapazitäten bis zu 2 TBit pro Quadratzoll möglich. In den letzten neun Jahren hätten die Ingenieure jährlich eine Steigerung von 30 Prozent bei der Datendichte erreicht. 2019 sollen bereits Festplatten mit mindestens 20 TByte möglich sein, für 2023 erwartet Re bereits 40 TByte. Zur Erinnerung: Auch WD verspricht mit seiner Mikrowellen-Technik MAMR-Technik [40-TByte-Festplatten](#), aber erst zwei Jahre später.

Fully functional pre-series ready now with 16 TB...

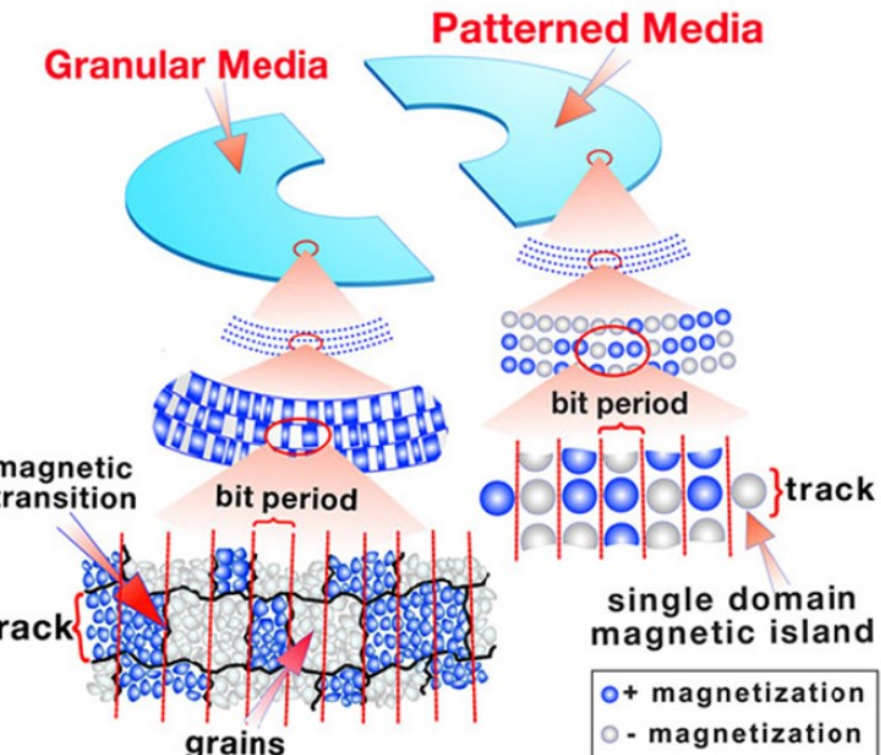
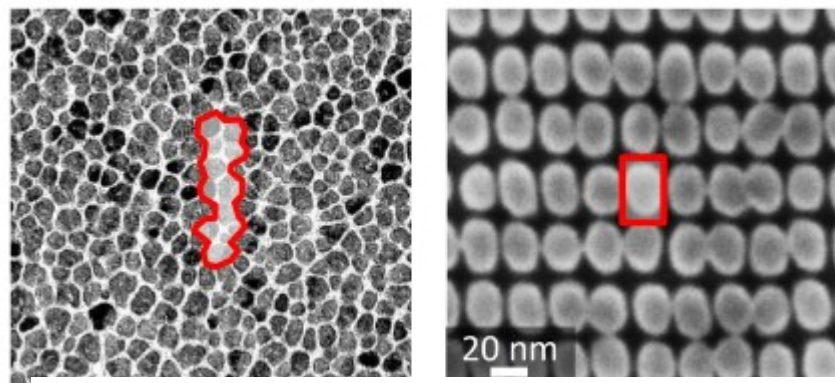
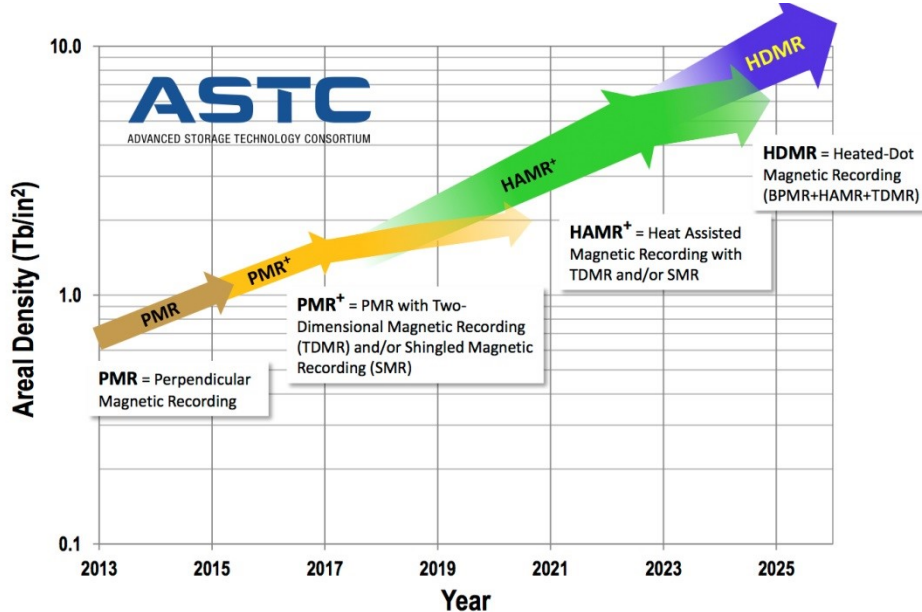
About 1 year delay with respect to last year's estimate, i.e., "100%"

→ Demanding from a technological point of view



Introduction to Magnetic Materials

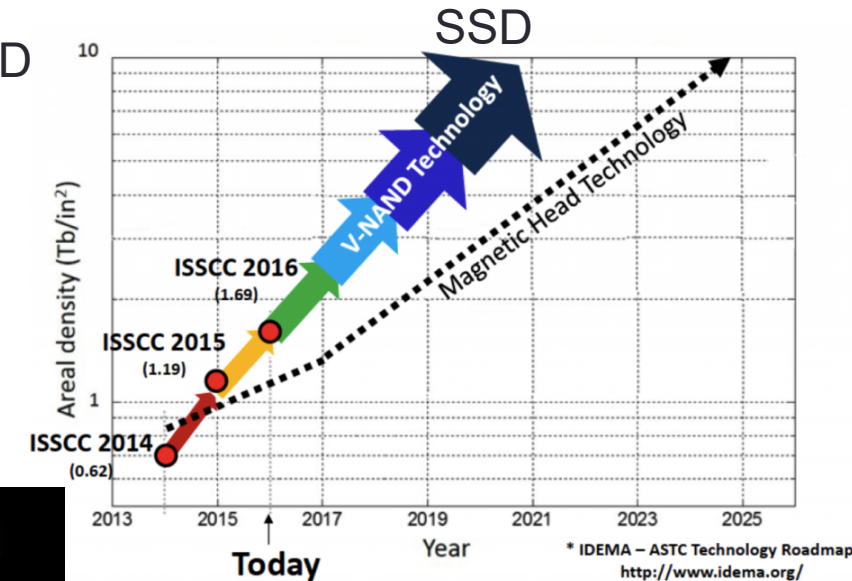
Temporal Evolution of Storage Density in HDD



Griffith et al., J. Phys. D: Appl. Phys. 46, 503001 (2013)

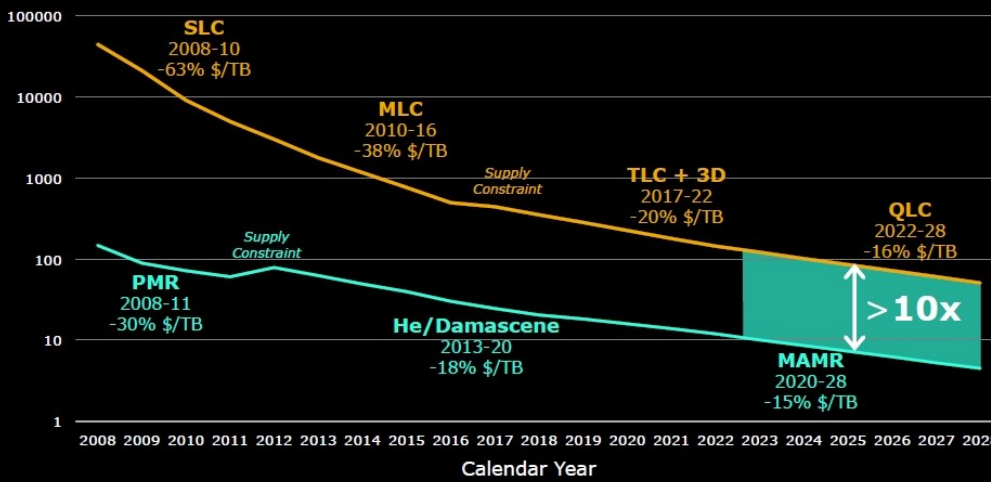
Introduction to Magnetic Materials

Temporal Evolution of Storage Density in HDD
HDD vs FLASH (SSD) memory



HDD vs. Flash SSD \$/TB Annual Takedown Trend

MAMR will enable continued \$/TB advantage over Flash SSDs



Is magnetism out of the game?



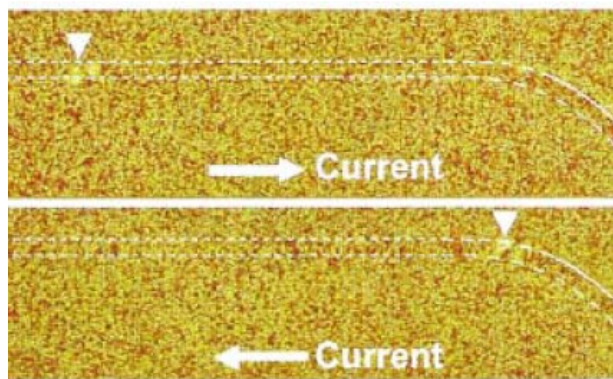
Introduction to Magnetic Materials

New Concepts Triggered by Novel Phenomena

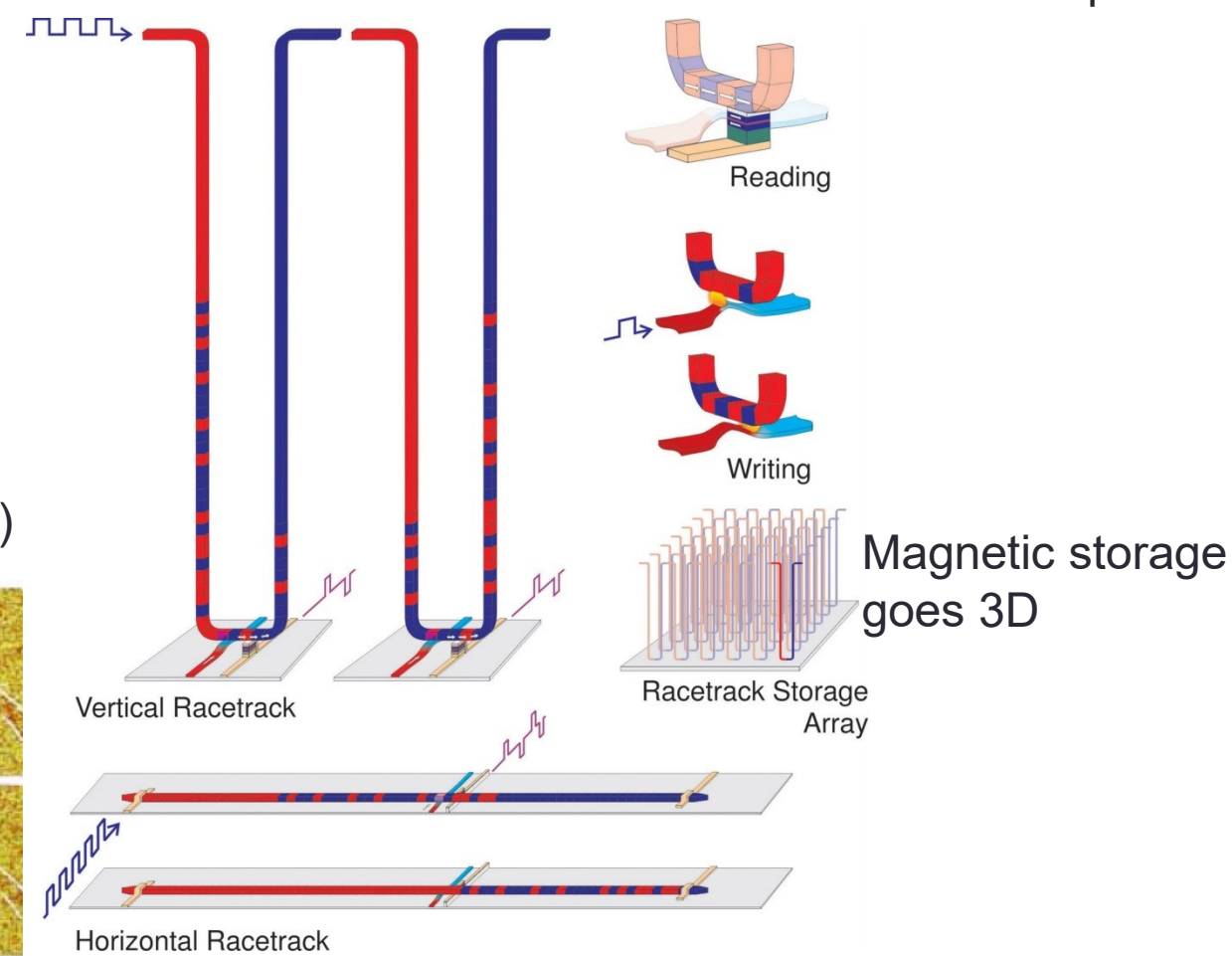
Racetrack Memory (2008)

Electrical currents can manipulate magnetism!

- Oersted fields (1820)
- Current Driven Domain Wall Motion due to Spin-Torque Phenomena (2004)



A. Yamaguchi et al., Phys. Rev. Lett. 92, 077205 (2004)



S.S.P. Parkin et al., Science 320, 5873 (2008)

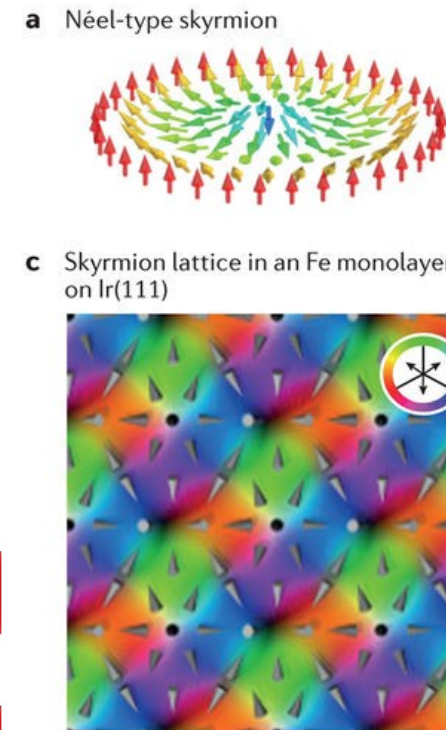
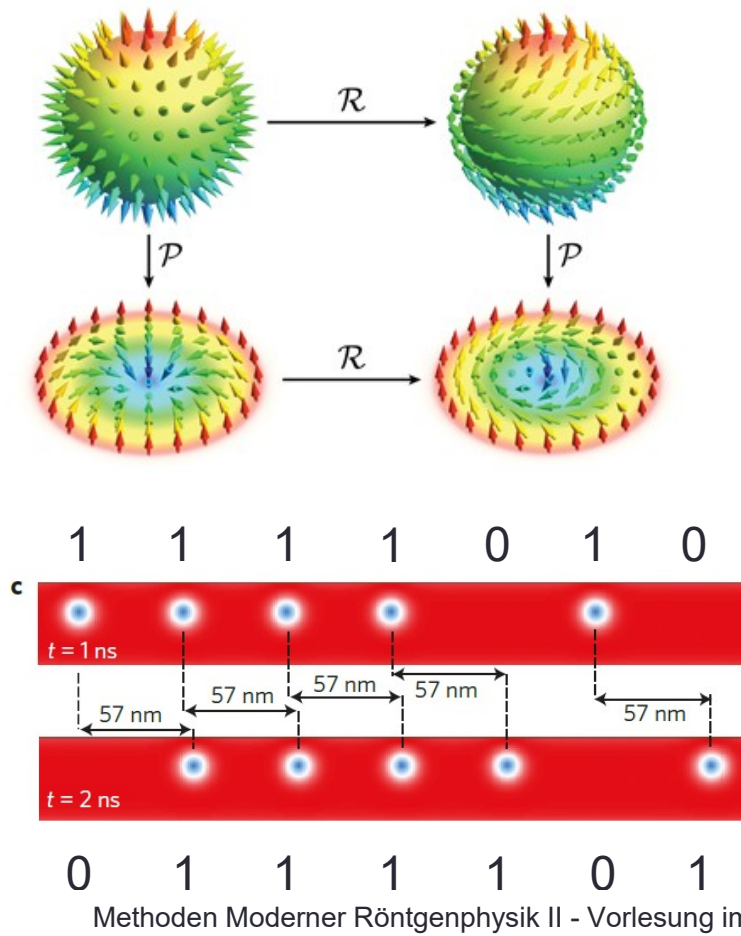
Methoden Moderner Röntgenphysik II - Vorlesung im Haupt-/Masterstudiengang, Universität Hamburg, SoSe 2019,
Leonard Müller



Introduction to Magnetic Materials

New Concepts Triggered by Novel Phenomena

Skyrmion Racetrack Memory (2013)



A. Fert et al., Nat. Nanotech. 8, 152 (2013)

A. Fert et al., Nature Rev. Mat. 2, 17031 (2017)

Nature Reviews | Materials

Methoden Moderner Röntgenphysik II - Vorlesung im Haupt-/Masterstudiengang, Universität Hamburg, SoSe 2019,
Leonard Müller



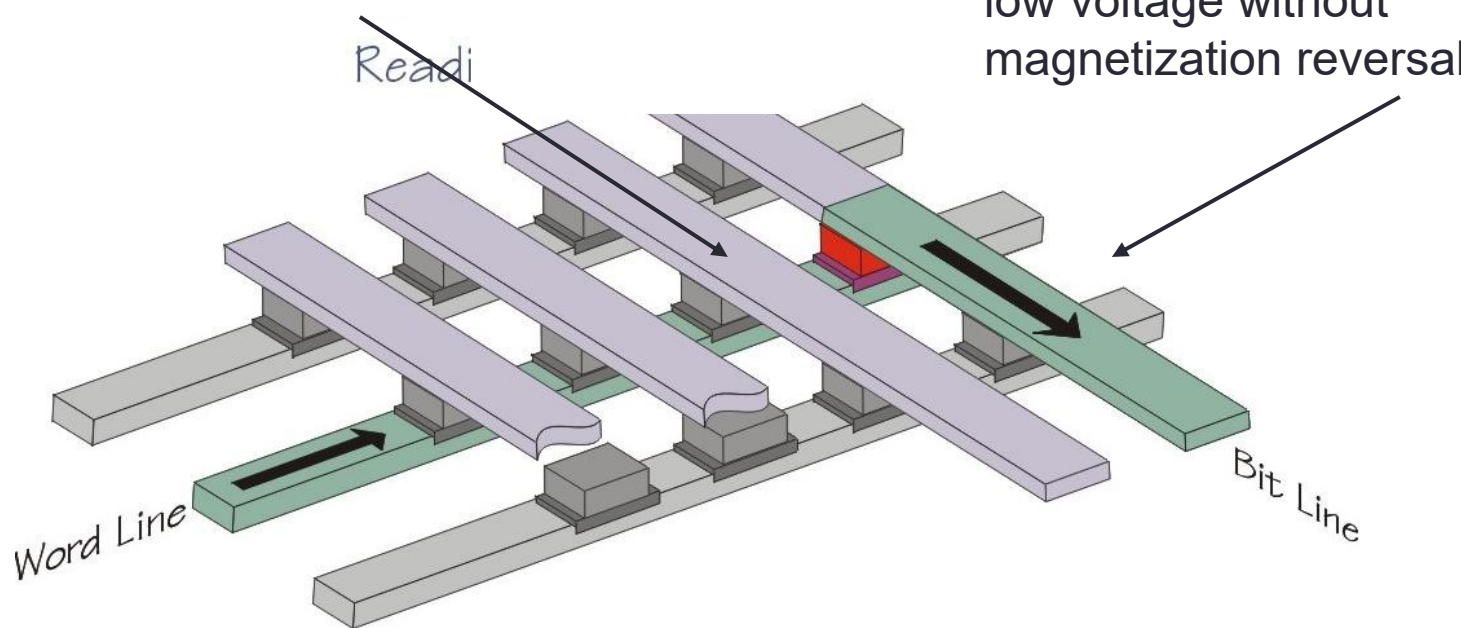
Introduction to Magnetic Materials

New Concepts triggered by novel Phenomena

(Non-Volatile) Magnetic Random Access Memory (MRAM)

Nanoscale:
1dot = 1bit

Read by means of
low voltage without
magnetization reversal

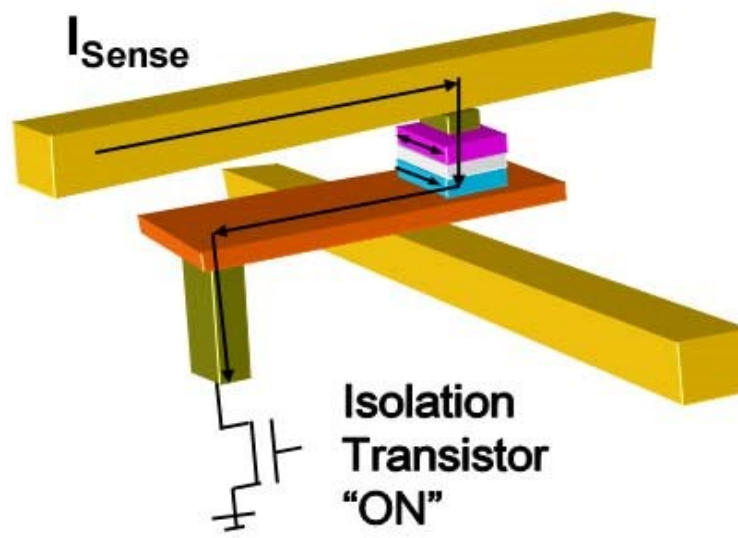


Dot size $20 \times 20 \text{ nm}^2$, distance 20nm: 4 Tbit/inch 2

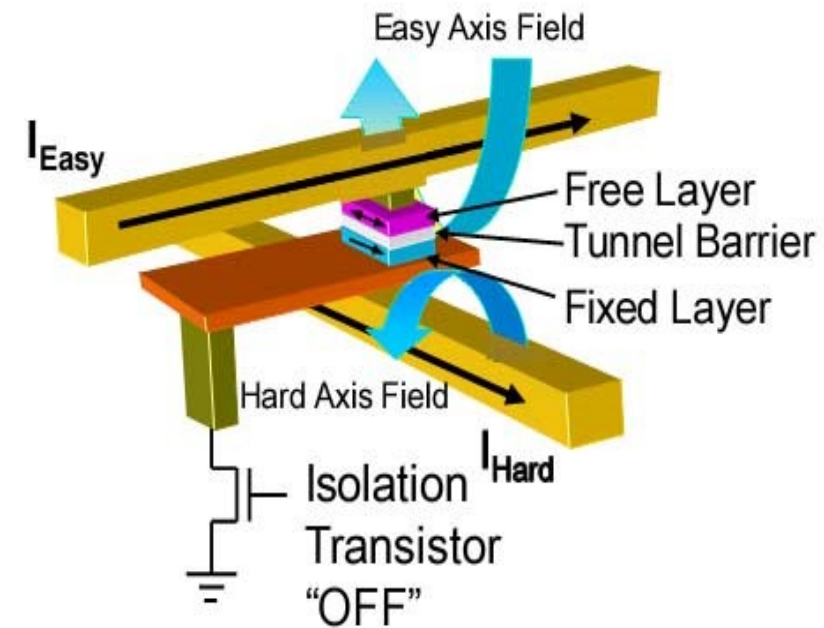
Introduction to Magnetic Materials

New Concepts triggered by novel Phenomena

(Non-Volatile) Magnetic Random Access Memory (MRAM)



“Read” mode



“Write” mode

Bilder: „Freescale“

Introduction to Magnetic Materials

New Concepts triggered by novel Phenomena

(Non-Volatile) Magnetic Random Access Memory (MRAM)

EVERSPIN® TECHNOLOGIES

About Everspin Investors Careers Press 

PRODUCTS APPLICATIONS

Home > DDR4 ST-MRAM Product

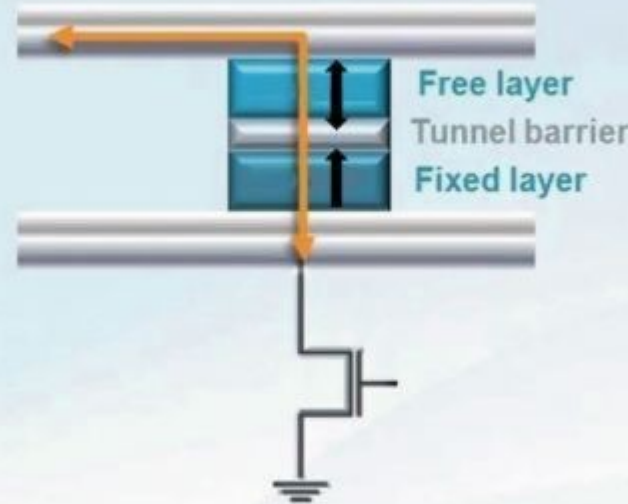
DDR4 ST-MRAM

DDR4 Compatible Sp

Everspin's newest Spin-Torque RAM is DDR4 compatible with some timing differences that:

- DDR4 protocol and physical interface
- Non-volatile, high endurance
- Capable of operation at higher temperatures
- Refresh is not required via self-refresh
- Some unique timing and control requirements

Spin Torque Write with pMTJ



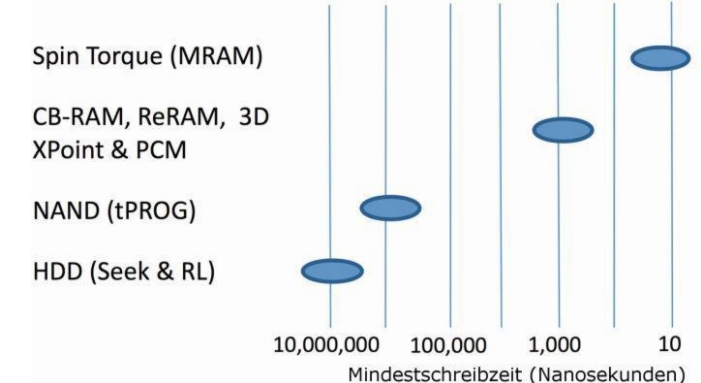
Free layer
Tunnel barrier
Fixed layer

Everspin 1Gb DDR4 Spin

The EMD4E001G is a 1 Gigabit ST-MRAM device designed for DDR4 operation at rates of up to 2666 MHz.

[Request more information about this product](#)

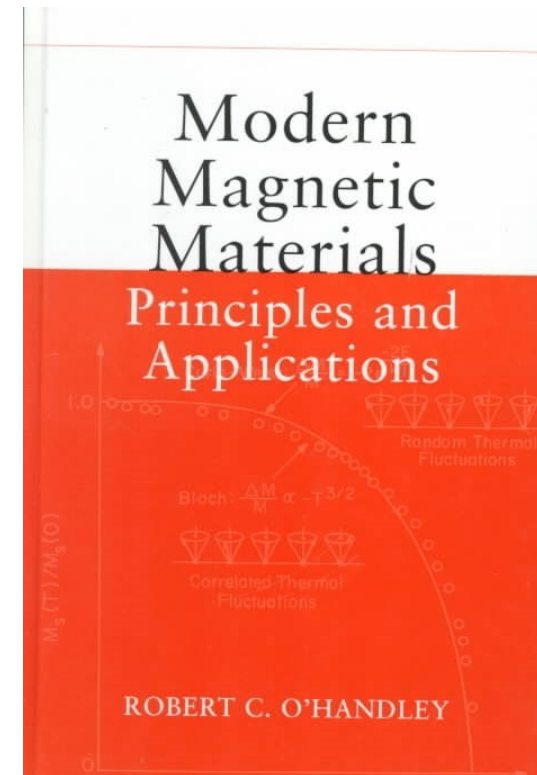
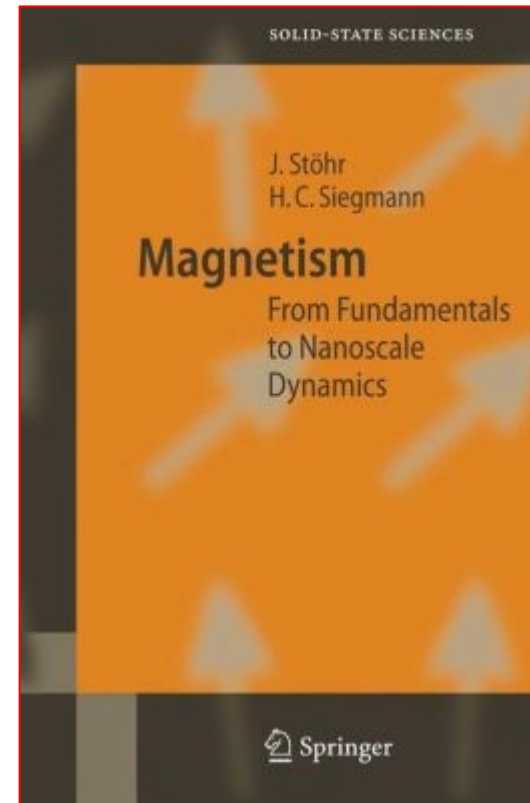
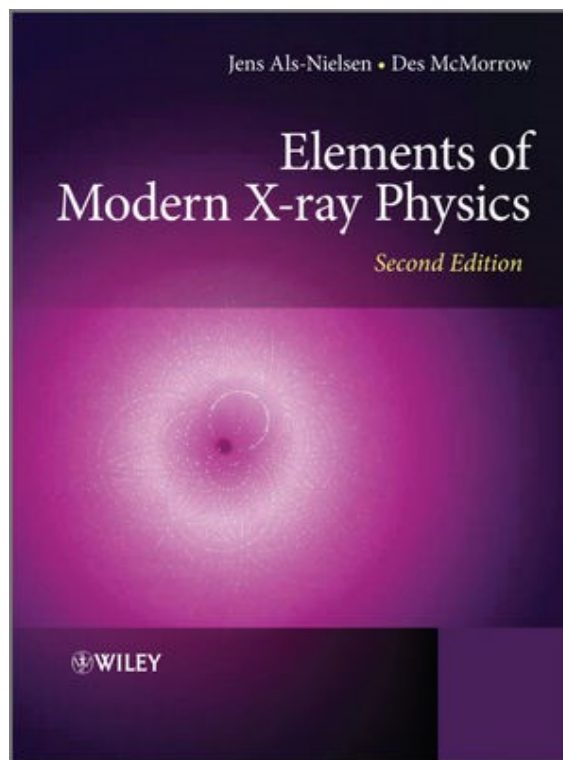
- **Höhere Effizienz der Ummagnetisierung erfordert weniger Strom**
- **Hohe Wiederbeschreibbarkeit und Datenerhaltung**
- **Weiterentwickelte MTJ auf MgO/CoFeB-Basis**



“now”

MRAM is designed for enterprise-style applications like SSD buffers, RAID buffers or synchronous logging applications where endurance is a must. The persistence of STT-MRAM protects data and enables systems to dramatically reduce latency, by up to 10x, and driving both efficiency and cost savings.

Literature:



<http://magnetism.eu>

Methoden Moderner Röntgenphysik II - Vorlesung im Haupt-/Masterstudiengang, Universität Hamburg, SoSe 2019,
Leonard Müller



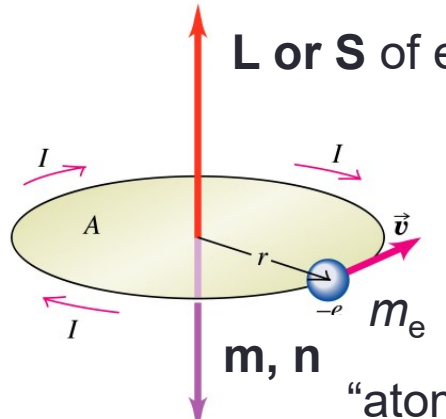
Introduction to Magnetic Materials

1.) Ferromagnetism in a nutshell

- Forms of Magnetic Phenomena
- Contributions to Magnetic Free Energy
- Focus on Systems with Perpendicular Magnetic Anisotropy (Co/Pt multilayers)
- Magnetic Domains and Domain Walls

Ferromagnetism in a nutshell – Forms of magnetism

- > Magnetic (dipole) moment \mathbf{m} (basic element of magnetism)



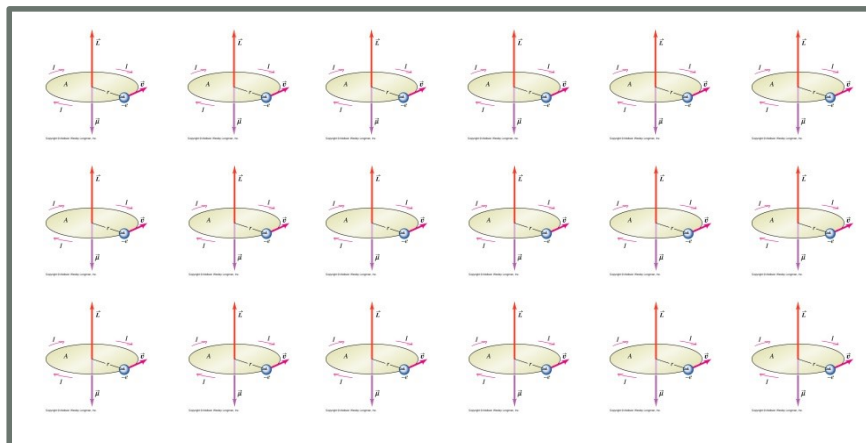
Copyright © Addison Wesley Longman, Inc.

Definition: $\mathbf{m} = I \cdot A \cdot \mathbf{n}$
 Unit: [m] = Am²

\mathbf{n} = surface normal of A

“atom” = conductor (or current) loop (Physik II)

- Magnetization: $\mathbf{M} = \sum \mathbf{m}/V$



Saturation magnetization (“length” of \mathbf{M}):

$$M_s = |\sum \mathbf{m}|/V$$

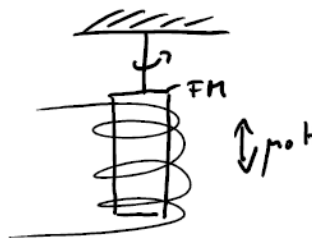
Volume V

Ferromagnetism in a nutshell – Forms of magnetism

- Connection to angular momentum \mathbf{L}

Current loop of moving charges with mass m_e exhibits angular momentum

$\mathbf{m} = \gamma \mathbf{L}$ γ : gyromagnetic ratio (proportionality proofed 1915 by Einstein-de Haas)



Torsion of string
is changed by mag.

Durch alle Messungen konnte übereinstimmend der „Einstein-Effekt“ nachgewiesen werden, aber in einer Größe, die nicht der zugrunde gelegten Theorie entspricht, nach welcher nur *negative* Elektronen mit dem Wert $m/e = 0,565 \cdot 10^{-7}$ in den magnetischen Molekülen kreisen. Während Einstein und de Haas auch quantitativ eine sehr gute Bestätigung der Theorie finden, ergeben meine Messungen einen bei Eisen um 47 Proz., bei Nickel um 43 Proz. zu kleinen Einstein-Effekt.

E. Beck, Ann. Phys. **18**, 1919 (1915)

$$|\vec{m}| = I \cdot A, \quad A = \text{area encircled by current}$$

$$|\vec{L}| = Nrmv, \quad N = \# \text{ particles}, v = \frac{2\pi r}{T}, I = \frac{qN}{T}, \quad T = \text{revolution time}$$

$$\frac{|\vec{m}|}{|\vec{L}|} = \frac{IA}{Nrmv}$$

Only for classical ring current; for spins there is an additional g (Landé factor)

Ferromagnetism in a nutshell – Forms of magnetism

Quantization of angular momentum \mathbf{L} in units of \hbar

→ Quantization of \mathbf{m} in units of Bohr magneton μ_B

$$|\vec{m}| = \gamma \hbar = \frac{q \hbar}{2m}, \text{ for } q = |e|: \quad \mu_B = 9.274 \cdot 10^{-24} \text{ Am}^2$$

Note that $\gamma < 0$ for electrons $\vec{L} \uparrow\downarrow \vec{m}$

Landé- or g- (or gyromagnetic-)factor: $\gamma = g \frac{q}{2m}$

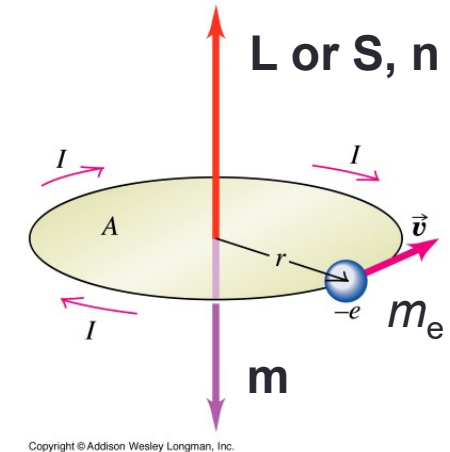
$g = 1$: classical description, anular momentum (orbital)

$g = 2.00231930436182(52)$ for electron spin (exp.) In accordance with theory!

$g_p = 5.585694702(17)$ for protons

$g_n = -3.82608545(90)$ for neutrons

$g_{^{14}\text{C}} = 0$ for carbon 14



Ferromagnetism in a nutshell – Forms of magnetism

- Forms of magnetic phenomena in solid states

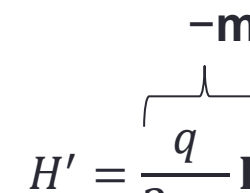
Diamagnetism and Paramagnetism

- Lorentz-force on moving charges in a magnetic field \mathbf{B} : $\mathbf{F} = q\mathbf{v} \times \mathbf{B}$

- Two further terms in Hamiltonian: $H = H_0 + H'$

- For one electron on circular loop (“atom”):

$$H' = \frac{q}{2m_e} \mathbf{L} \cdot \mathbf{B} + \frac{q^2}{8m_e} (\mathbf{B} \times \mathbf{r})^2$$





1.) Paramagnetic term

- energy of magnetic dipole in field
- alignment of \mathbf{m} with magnetic field \mathbf{B}
- T dependent (later)

Electron-orbit
Radius
(expect.
value)

2.) Diamagnetic term

- all materials are diamagnetic
- always > 0
- inhomogeneous field: atom can reduce energy when moving to region of lowest field
- T independent

Ferromagnetism in a nutshell – Forms of magnetism

- Different types of magnetic phenomena in solid states

Diamagnetism and Paramagnetism

- Ratio of both corrections:

$$\frac{\frac{q}{2m} \vec{L} \cdot \vec{B}}{\frac{q^2}{8m} |\vec{B} \times \vec{r}|^2} \geq \frac{\frac{\mu_B}{2m} \hbar B}{\frac{q^2}{8m} B^2 r^2} = \frac{4\hbar}{qBr^2} = 10^4 \quad \text{for } B = 10 \text{ T and } r = 0.15 \text{ nm}$$

- Comparison of paramagnetic term to thermal energy at room temp. for $B = 10 \text{ T}$:

$$\begin{aligned} E_{therm} &= 25 \text{ meV} = (k_B T) \\ E_{para} &= 0.58 \text{ meV} \end{aligned} \quad E_{para} \ll E_{therm}$$

- Thermodynamic description:

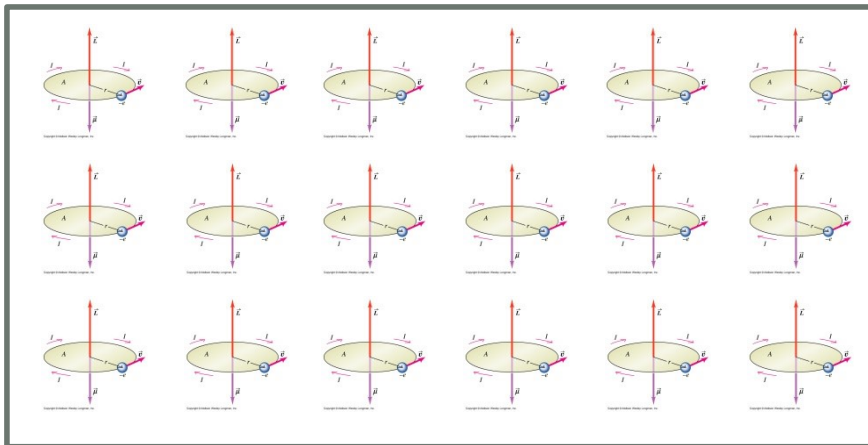
$$\frac{\langle m \rangle}{\mu_B} = \tanh \frac{\mu_B B}{k_B T} \approx \frac{\mu_B B}{k_B T} = \frac{E_{para}}{E_{therm}} = 0.023 \text{ at } 10 \text{ T}$$

Ferromagnetism in a nutshell – Forms of magnetism

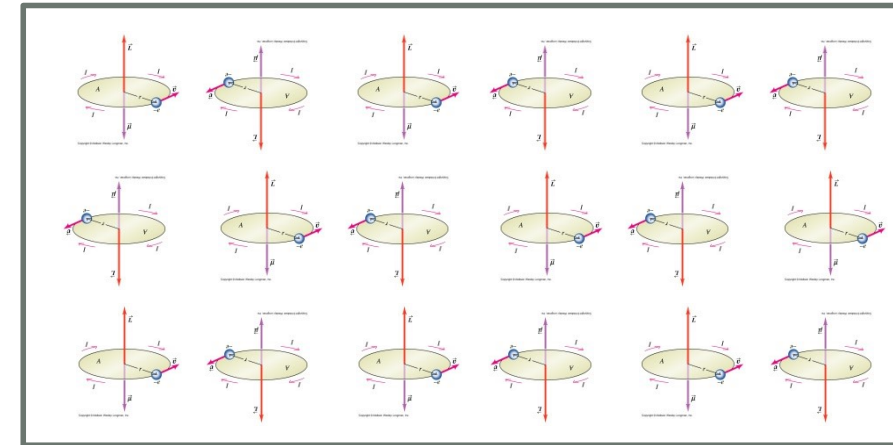
- > Different types of magnetic phenomena in solid states

Materials with long-range magnetic order (without external magnetic field)
due to strong interaction between electron's magnetic moments

Ferromagnetism (FM)



Antiferromagnetism (AFM)

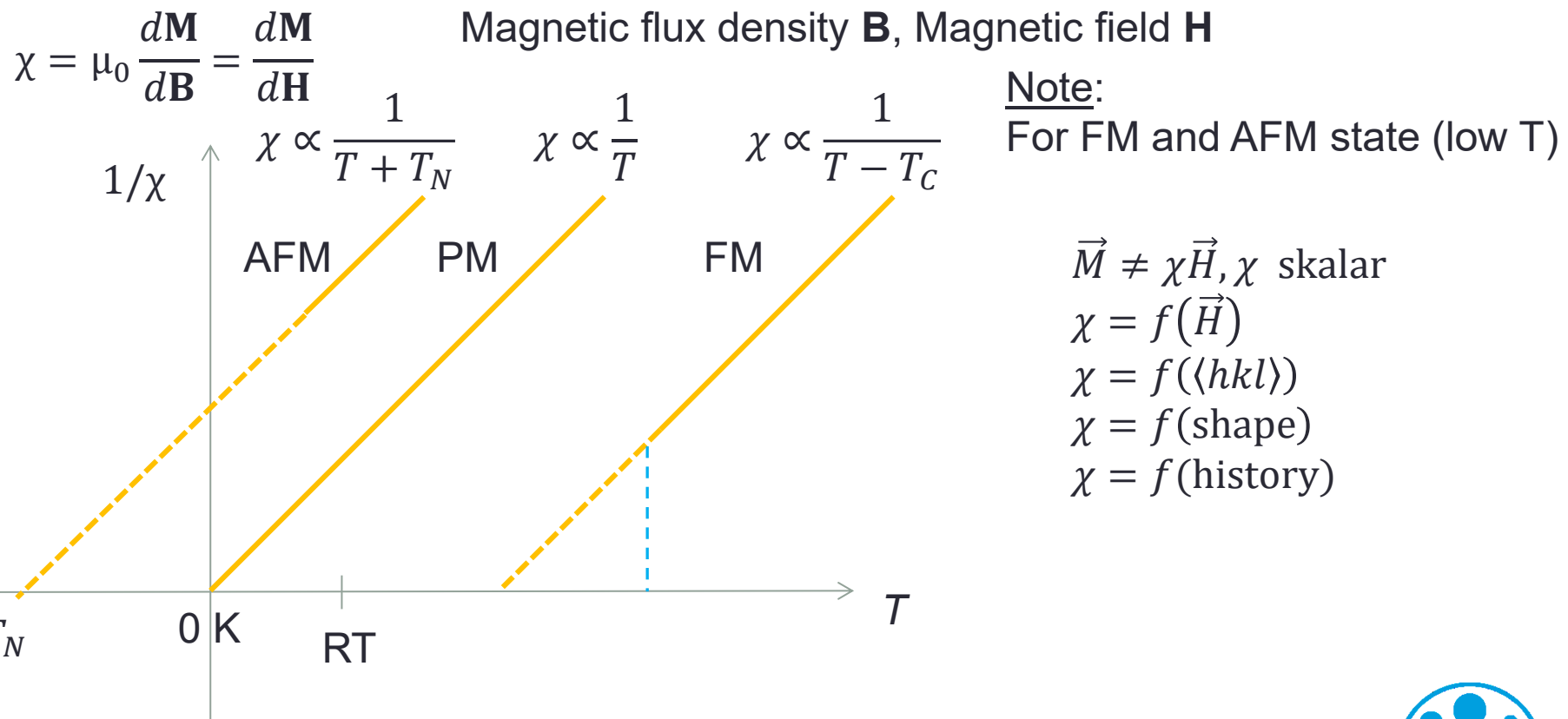


Classic description via mean field (Weiß 1907): $|\mathbf{B}_{xc}| = \mu_0 \lambda(J) |\mathbf{M}| = 10^3 \text{ T}!$

Ferromagnetism in a nutshell – Forms of magnetism

➤ Different types of magnetic phenomena $M = \frac{\partial E}{\partial B}, \quad \chi = -\mu_0 \frac{\partial^2 E}{\partial B^2}, \quad E = \text{free Energy}$

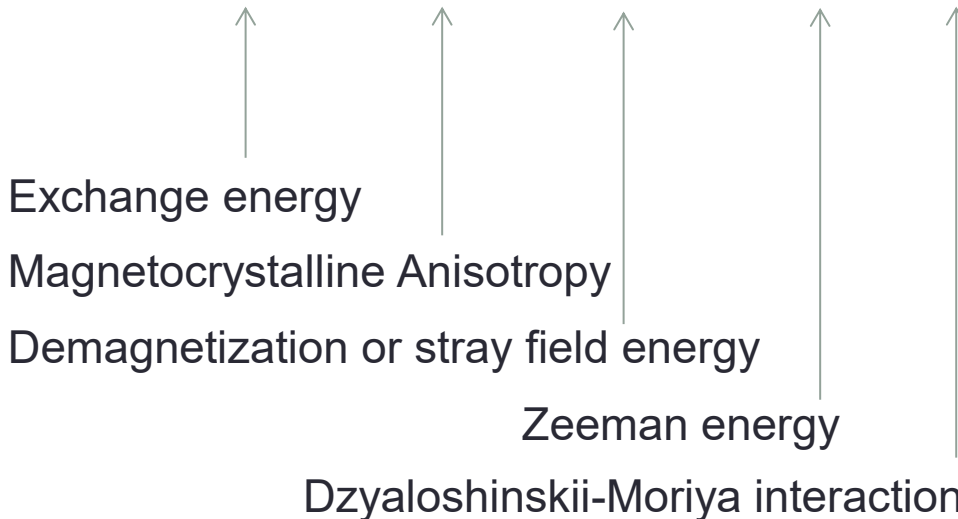
Classification by means of magnetic susceptibility χ , i.e., response of magnetization to magnetic field (in high T regime, i.e., above a critical temperature):



Ferromagnetism in a nutshell – Magnetic energies

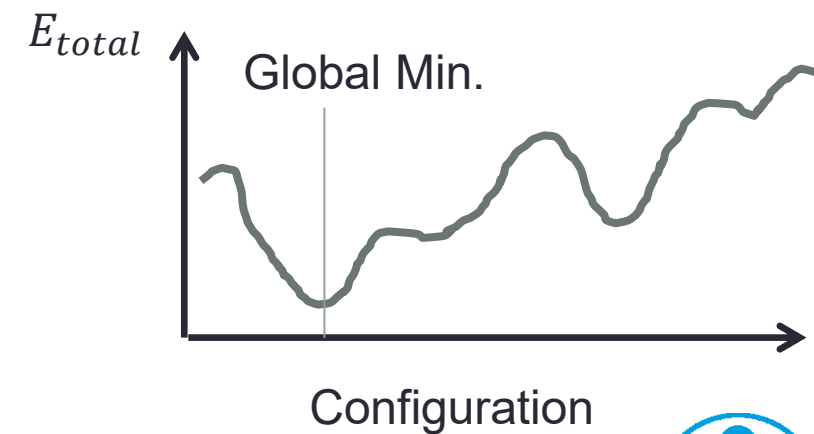
> Magnetic free energy

$$E_{\text{total}} = E_{\text{XC}} + E_{\text{MCA}} + E_{\text{demag}} + E_{\text{Zeeman}} + E_{\text{DMI}} + \dots$$



In equilibrium:

$$\frac{dE}{dm_i} = 0 \\ (\frac{d^2E}{dm_i^2} > 0)$$



Ferromagnetism in a nutshell – Magnetic energies

> Exchange energy

- Origin:

1.) Coulomb interaction between electrons

$$H_{\text{Coulomb}} = \frac{1}{2} \sum_{i \neq j} \frac{e^2}{4\pi\epsilon_0 r_{ij}}$$

2.) Pauli's exclusion principle: Total wave function $|\phi\rangle = |\Psi\rangle \cdot |\chi\rangle$ is antisymmetric when interchanging two identical = undistinguishable particles

$$J \propto \langle \Psi_{\text{symmetric}} | H_{\text{Coulomb}} | \Psi_{\text{symmetric}} \rangle - \langle \Psi_{\text{antisymmetric}} | H_{\text{Coulomb}} | \Psi_{\text{antisymmetric}} \rangle$$

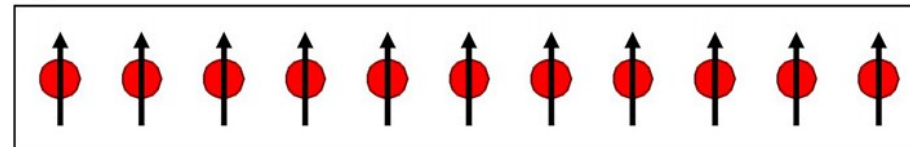
↑
Exchange constant (or integral)

Spatial wave function

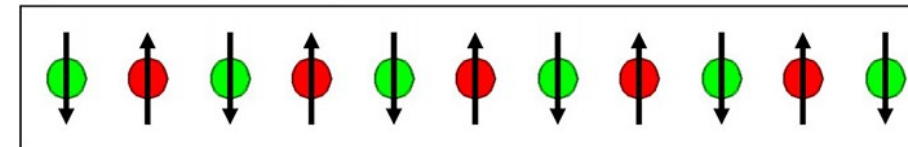
→ Heisenberg exchange (effective spin-spin interaction)
 (generally, only next neighbor interaction)

$$E_{\text{XC}} = - \sum_{i \neq j} J_{ij} \mathbf{s}_i \cdot \mathbf{s}_j$$

$J_1 > 0$ ferromagnetic

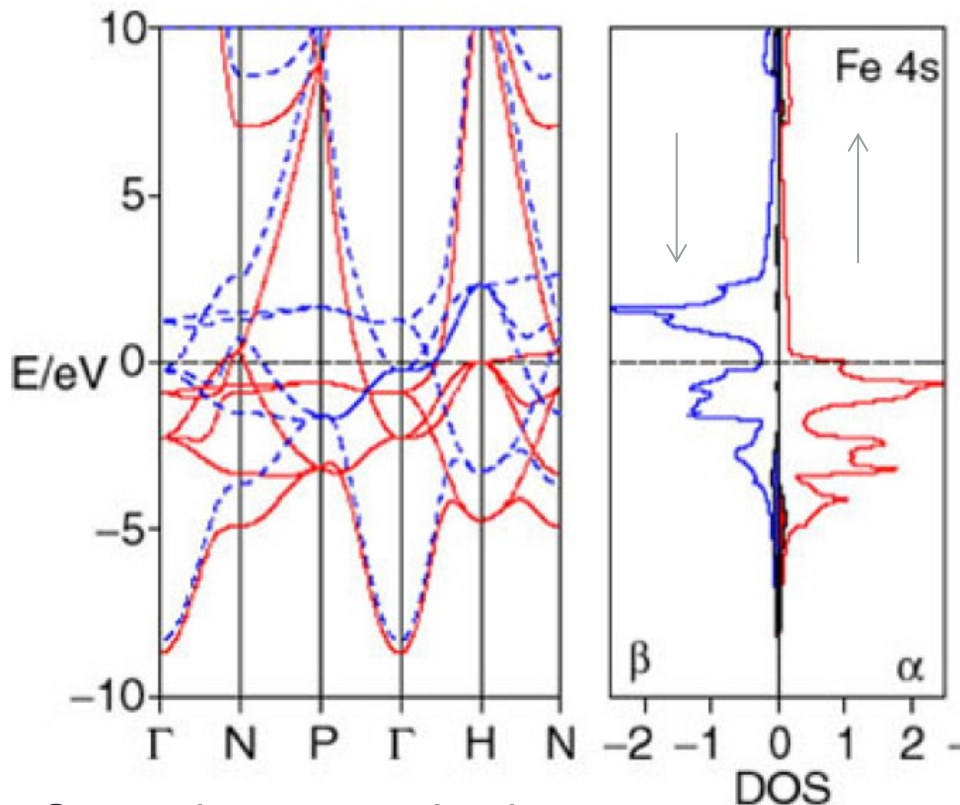


$J_1 < 0$ antiferromagnetic

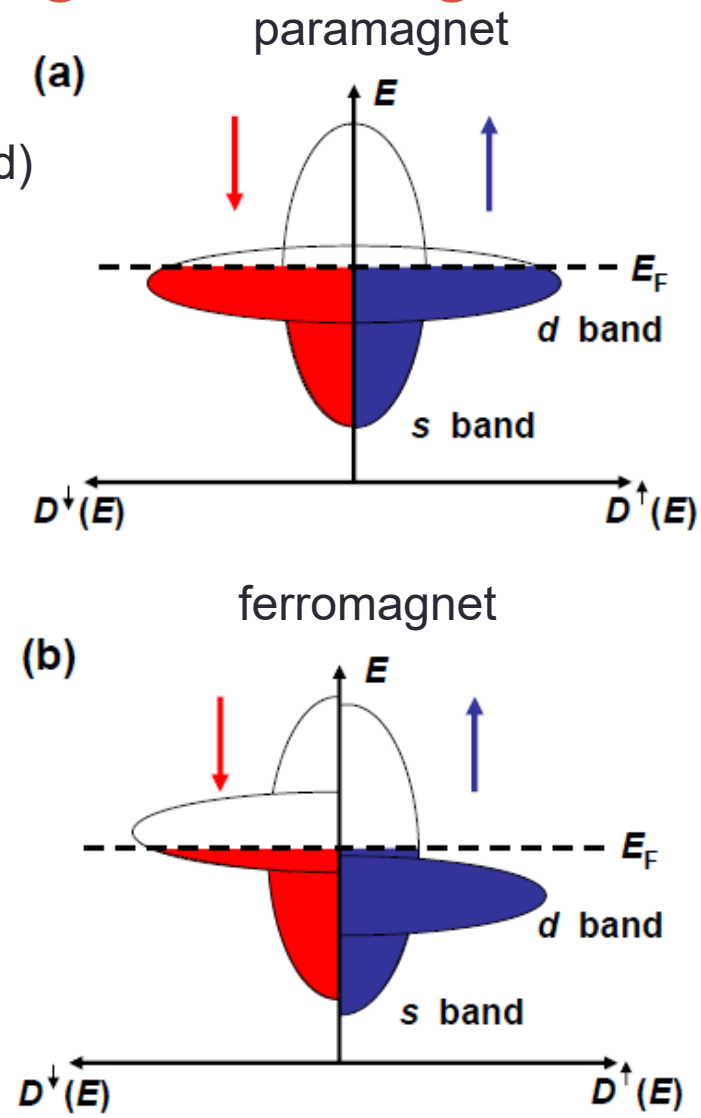


Ferromagnetism in a nutshell – Magnetic energies

- Itinerant (band) Ferromagnetism for Ni, Fe, Co
(≠ localized FM for rare-earth elements like Dy, Tb, Gd)



- Saturation magnetization: $M_S = \mu_B(n_\uparrow - n_\downarrow)$



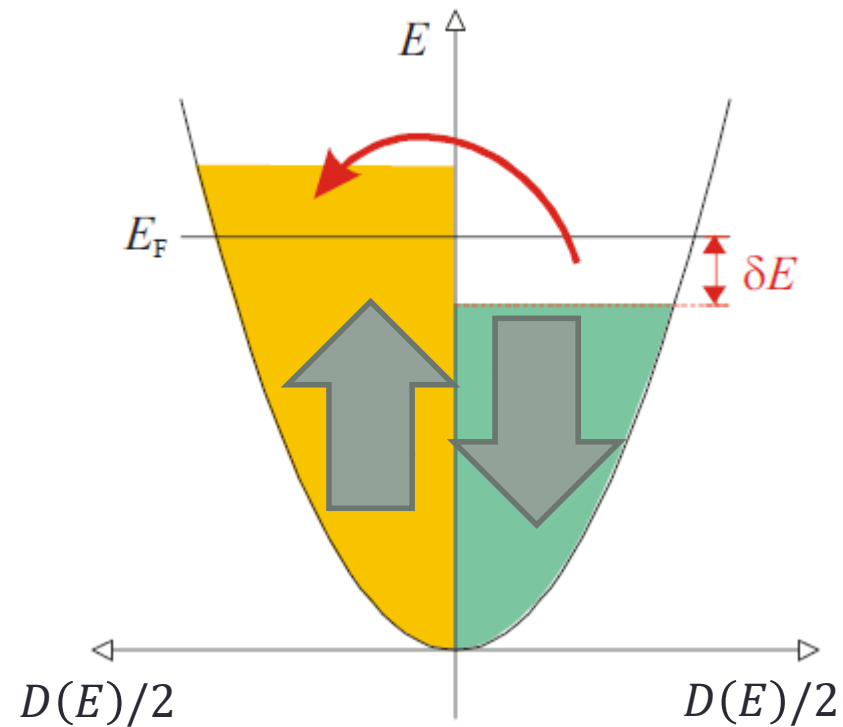
Ferromagnetism in a nutshell – Magnetic energies

- Itinerant (band) Ferromagnetism for Ni, Fe, Co
(assume quasi-free electron gas)

- Saturation magnetization: $M_S = \mu_B(n_\uparrow - n_\downarrow) = \mu_B D(E_F)\delta E$

Derivation:

$$n^{\uparrow\downarrow} = \frac{1}{2} \cdot (n \pm D(E_F) \cdot \delta E)$$



Ferromagnetism in a nutshell – Magnetic energies

➤ Itinerant (band) Ferromagnetism

Stoner criterion (1939): $I \cdot D(E_F) > 1$

I : Stoner parameter

- Derivation: Comparison of ferromagnet to paramagnet

1.) Increase of kinetic energy: $\Delta E_{\text{kin}} = \frac{D(E)\delta E}{2} \delta E$

Number of electrons

shift

2.) Decrease of static energy: $dE = -\mu_0 M dH_{\text{xc}} = -\mu_0 M \lambda(J) dM$

$$\begin{aligned}\Delta E_{\text{pot}} &= - \int_0^{M_S} M \mu_0 \lambda(J) dM = -\frac{\mu_0}{2} \lambda(J) M^2 S \\ &= -\frac{1}{2} \underbrace{\lambda(J) \mu_0 \mu_B^2}_{I} (D(E_F) \delta E)^2\end{aligned}$$

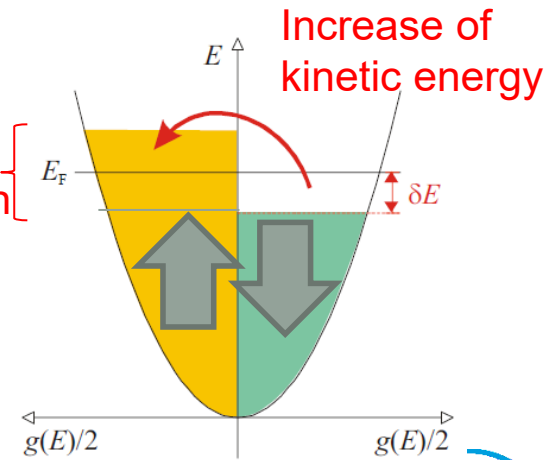
e⁻ without repulsive Coulomb interaction

3.) Total energy balance:

$$\Delta E = \Delta E_{\text{pot}} + \Delta E_{\text{kin}} = \frac{1}{2} D(E_F) \delta E^2 (1 - I \cdot D(E_F))$$

Ferromagnet if $\Delta E < 0 \Rightarrow I \cdot D(E_F) > 1$

	$n^\circ(E_F)[eV^{-1}]$	$I[eV]$	$I n^\circ(E_F)$
Na	0.23	1.82	0.41
Al	0.21	1.22	0.25
Cr	0.35	0.76	0.27
Mn	0.77	0.82	0.63
Fe	1.54	0.93	1.43
Co	1.72	0.99	1.70
Ni	2.02	1.01	2.04
Cu	0.14	0.73	0.11
Pd	1.14	0.68	0.78
Pt	0.79	0.63	0.50



Ferromagnetism in a nutshell – Magnetic energies

> magnetocrystalline anisotropy

- Gedankenexperiment:

Assume an infinite amorphous material (a)/ crystal (b), which orientation has **M**?

(a) All spins are aligned in parallel (**M** exists) due to exchange interaction but the direction of **M** is fluctuating

(b) Crystal field theory: Crystal order breaks isotropy

+ (Quenched) orbital momentum **L** is firmly linked to crystal lattice

+ **Spin orbit interaction** proportional to $\mathbf{L} \cdot \mathbf{S}$

→ Energy depends on orientation of **M** with respect to the crystal axes
= magnetocrystalline anisotropy

Ferromagnetism in a nutshell – Magnetic energies

> magnetocrystalline anisotropy

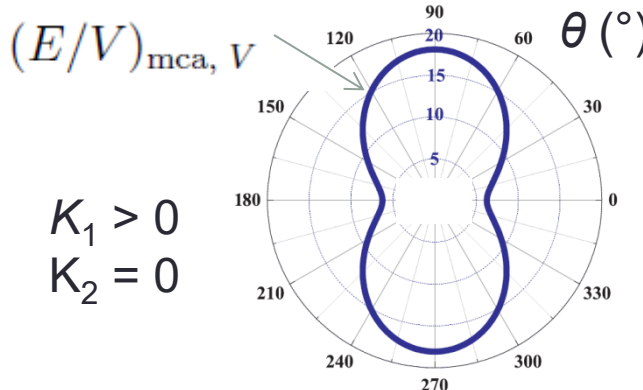
- Most simple case: *Uniaxial* MCA like in hcp crystals (e.g. Co at room temperature)

$$(E/V)_{\text{mca}, V} = K_{1V} \sin^2 \theta + \underline{K_{2V} \sin^4 \theta} + \mathcal{O}(\sin^6 \theta)$$

Higher order is also considered in the excercise

$K_{1V, \text{Co}} = +0.5 \text{ MJ/m}^3$ (three orders of magnitude smaller than XC)

→ The (0001) axis is the „easy axis of magnetization“ for Co



See today's excercise

$$K_1 < 0, K_2 = 0$$

$$-2K_2 < K_{10}, K_2 > 0$$

- Note: Magnetoelastic anisotropy due to lattice strain yields higher anisotropy constants, e.g., $K_V = 2.5 \text{ MJ/m}^3$ for tetragonally distorted FePt L1₀ alloys



Ferromagnetism in a nutshell – Magnetic energies

- (magnetocrystalline) interface anisotropy (Néel's pair interaction model 1959)

- origin: Symmetry breaking at interface as atoms at interfaces have less nearest neighbors of the same element

$$(E/V)_{\text{mca}, S} = \frac{2K_S \sin^2 \theta}{t}$$

$$E_{\text{MCA,total}}/V = (K_V + 2K_S/t) \sin^2 \theta$$

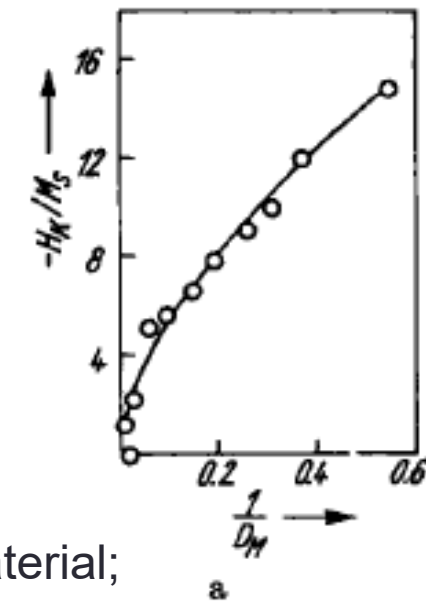
- Discovery by Gradmann and Müller for NiFe(111) on Cu (1968)

- Strongly depends on interface orientation and paramagnetic material; high positive value for Co(0001)/Pt(111); discovered 1988:

$$K_{S, \text{Co/Pt}} = +1 \text{ mJ/m}^2 \sim 10 \text{ MJ/m}^3 \text{ (two orders of magnitude smaller than XC interaction)}$$

↑
when considering half atomic layer (1Å)

- ➔ The (0001) axis is the „easy axis of magnetization“ for Co/Pt for small t



Ferromagnetism in a nutshell – Magnetic energies

- Demagnetization energy E_d (shape anisotropy)
 - Gedankenexperiment II:
What happens when cutting out a thin slice of an infinite ferromagnet?
- ➔ (crystalline materials: magnetocrystalline interface anisotropy)
- ➔ Generation of surface charges and demagnetization energy (positive definite) when \mathbf{M} has components along surface normal
- ➔ \mathbf{M} prefers to align along the surface (pole avoidance principle)
- ➔ (again) “easy and hard axis of magnetization“

$$\vec{B} = \mu_0(\vec{H} + \vec{M})$$

Ferromagnetism in a nutshell – Magnetic energies

> Demagnetization energy E_d

=Consequence of Maxwell equation:

$$\operatorname{div} \mathbf{B} = \mu_0 \operatorname{div} (\mathbf{M} + \mathbf{H}_d) = 0$$

$$E_{\text{ms}} = -\frac{\mu_0}{2} \int_V \mathbf{M} \cdot \mathbf{H}_d \, dV$$

$$\mathbf{H}_d = -\overleftrightarrow{N} \cdot \mathbf{M}$$

Rotational ellipsoids (single domain state):

Symmetry considerations:

$$\overleftrightarrow{N}_{\text{sphere}} = \begin{pmatrix} \frac{1}{3} & 0 & 0 \\ 0 & \frac{1}{3} & 0 \\ 0 & 0 & \frac{1}{3} \end{pmatrix}, \quad \overleftrightarrow{N}_{\text{wire}} = \begin{pmatrix} 0 & 0 & 0 \\ 0 & \frac{1}{2} & 0 \\ 0 & 0 & \frac{1}{2} \end{pmatrix}, \quad \overleftrightarrow{N}_{\text{film}} = \begin{pmatrix} 0 & 0 & 0 \\ 0 & 0 & 0 \\ 0 & 0 & 1 \end{pmatrix}$$


 Isotropy
 → No shape
 anisotropy

cylindrical wire ~ “cigar”

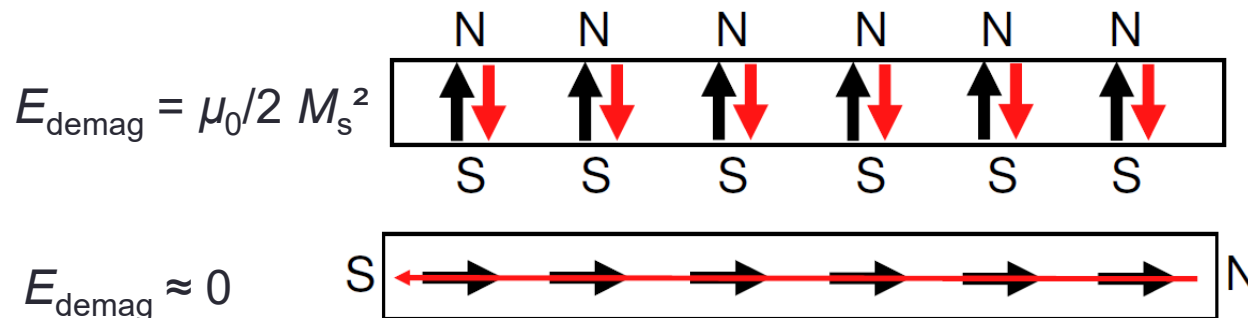
pancake



Ferromagnetism in a nutshell – Magnetic energies

➤ Demagnetization energy E_d

$$(E/V)_{d, \text{film}} = \frac{\mu_0}{2} (\vec{N}_{\text{film}} \cdot \mathbf{M}) \cdot \mathbf{M} = \frac{\mu_0}{2} M_z^2 = \frac{\mu_0}{2} M_s^2 \cos^2 \Theta$$



Redefinition of zero: $(E/V)_{d, \text{film}} = \frac{\mu_0}{2} M_s^2 \cos^2 \Theta = -\frac{\mu_0}{2} M_s^2 \sin^2 \Theta + \text{const.}$

$$(E/V)_d = -\mu_0/2 M_s^2 \sin^2 \theta = K_d \sin^2 \theta$$

For Co at room temperature: $M_s = 1.44 \text{ MA/m} \rightarrow$
 $K_d = -\mu_0 M_s^2 / 2 = -1.3 \text{ MJ/m}^3$

Ferromagnetism in a nutshell – Magnetic energies

- Effective anisotropy constant for uniaxial thin films:

$$K_{1,\text{eff}} = \underbrace{K_{1V}}_{K_{1V,\text{eff}}} - \frac{\mu_0}{2} M_S^2 + \frac{2K_{1S}}{t}$$

For Co(0001)/Pt(111) system:

$$K_d = -1.3 \text{ MJ/m}^3$$

$$K_{1V} = +0.5 \text{ MJ/m}^3$$

$$K_{1S} = +1 \text{ mJ/m}^2$$

Easy axis
out-of-plane!

M

Easy plane
behavior

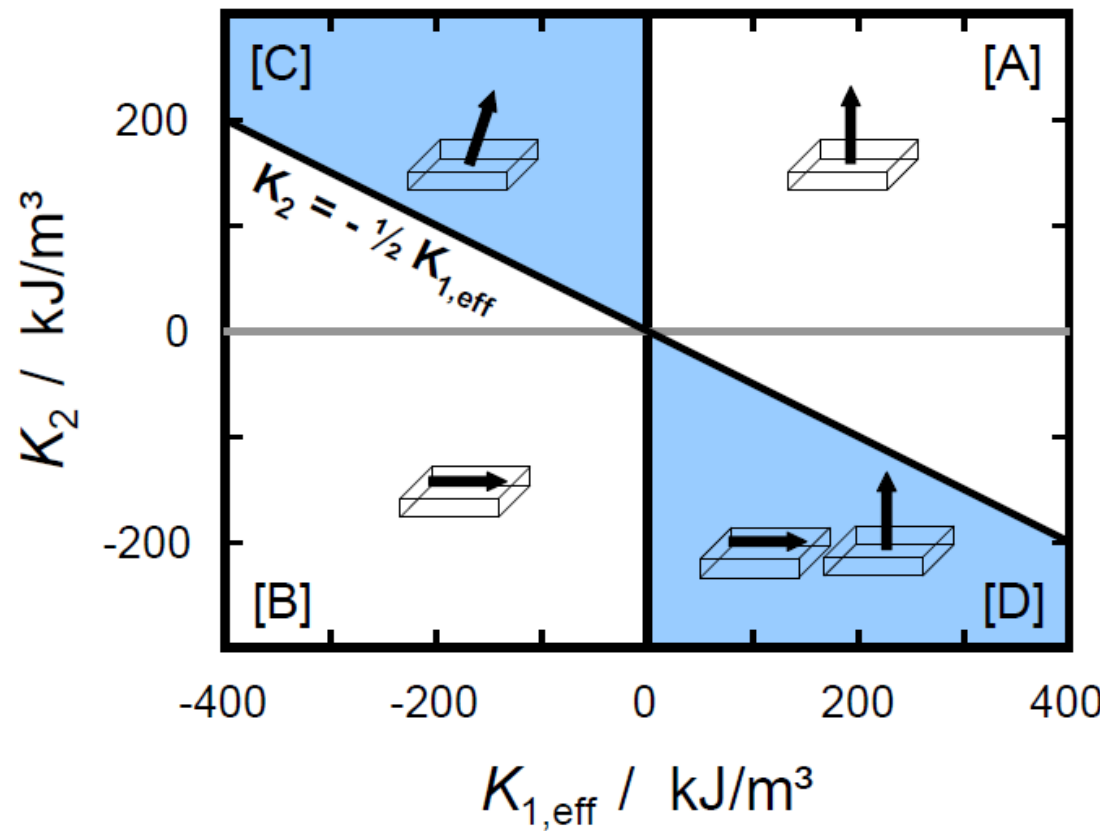
M

→ $K_{1,\text{eff}} > 0$ for $t < 2 \text{ nm}$!!!

$K_{1,\text{eff}} < 0$ for $t > 2 \text{ nm}$

Ferromagnetism in a nutshell – Magnetic energies

- Phase diagram (considering higher orders in anisotropy constants; today's excercise)



Ferromagnetism in a nutshell – Magnetic energies

> Zeeman energy

=Energy of magnetization \mathbf{M} in external magnetic field \mathbf{H}

$$(E/V)_Z = -\mu_0 \mathbf{M} \cdot \mathbf{H}$$

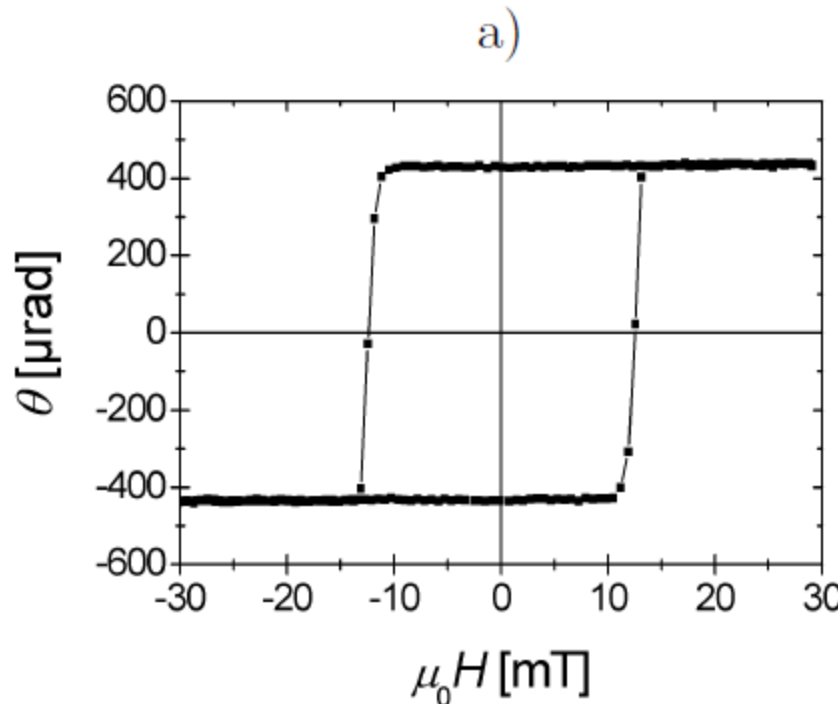
> Total energy of single-domain system (today's Übung):

$$E/V = \underbrace{K_{1,\text{eff}} \sin^2 \Theta + K_2 \sin^4 \Theta}_{\text{MCA+shape anisotropy terms}} - \mu_0 H M_S \cos \Phi$$

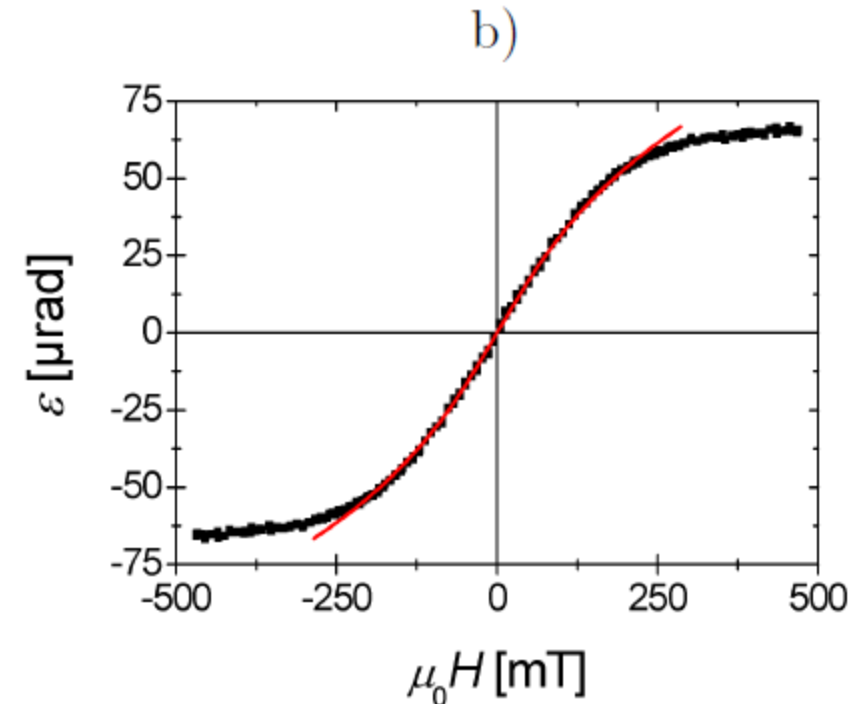
↑
Zeeman term

Ferromagnetism in a nutshell – Magnetic energies

> Magnetic hysteresis curves



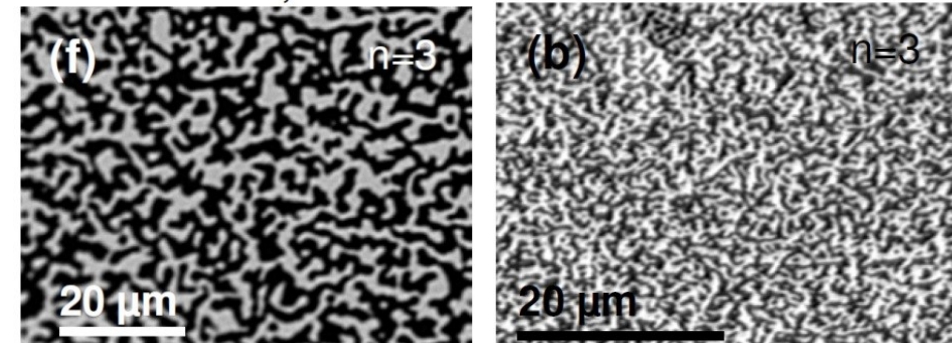
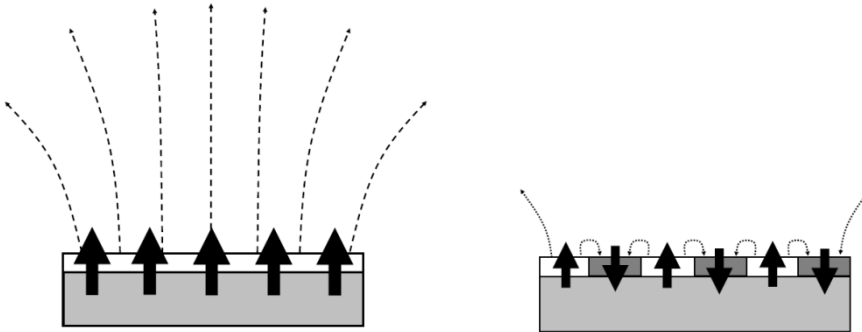
Easy axis
(domain nucleation and domain wall motion)



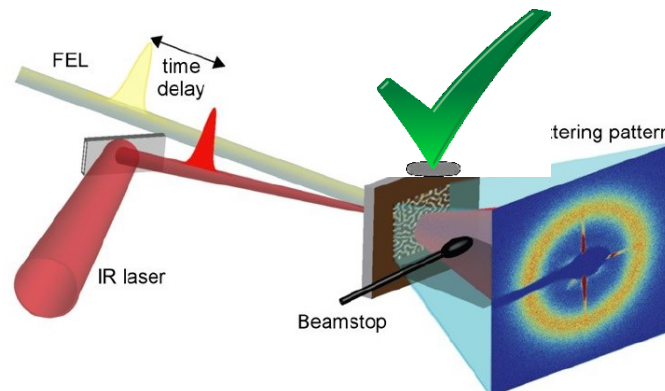
Hard axis
(coherent rotation of magnetization,
today's excercise)

Ferromagnetism in a nutshell – Domains and Walls

> Magnetic domains and domain walls



- Domain walls cost exchange E_{XC} and magnetocrystalline anisotropy energy E_{MCA}
- But: Domain formation reduces stray field energy E_d



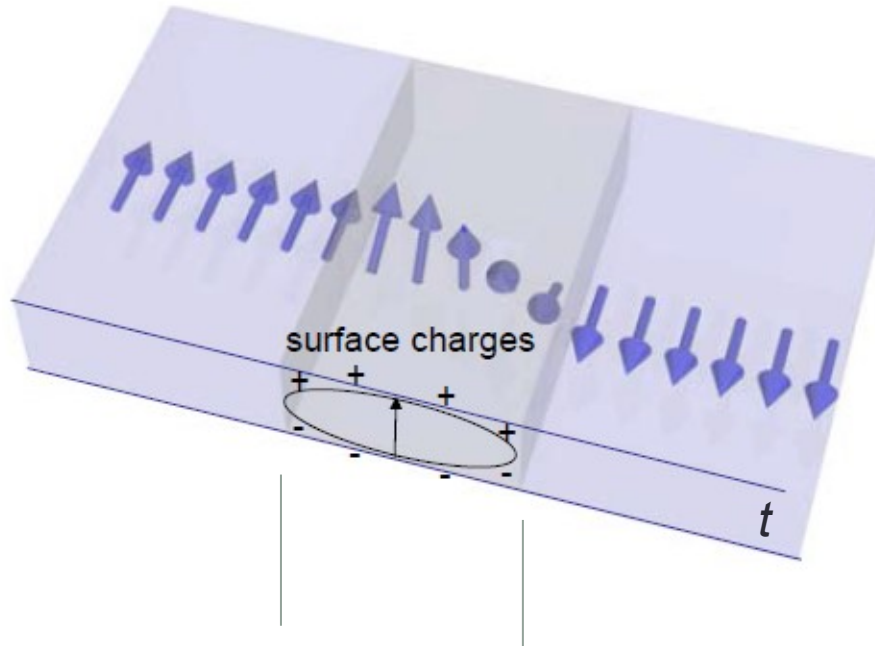
B. Pfau et al., *Nature Communications*, Vol. 3, 11; DOI:doi:10.1038/ncomms2108 (2012)
I. Müller et al. *Rev. Sci. Instrum.* 84 013906 (2013)

With x-rays, under certain conditions, up and down domains are more or less opaque and hence yield scattering contrast. Magnetic structure can be investigated on the nanoscale

Ferromagnetism in a nutshell – Domains and Walls

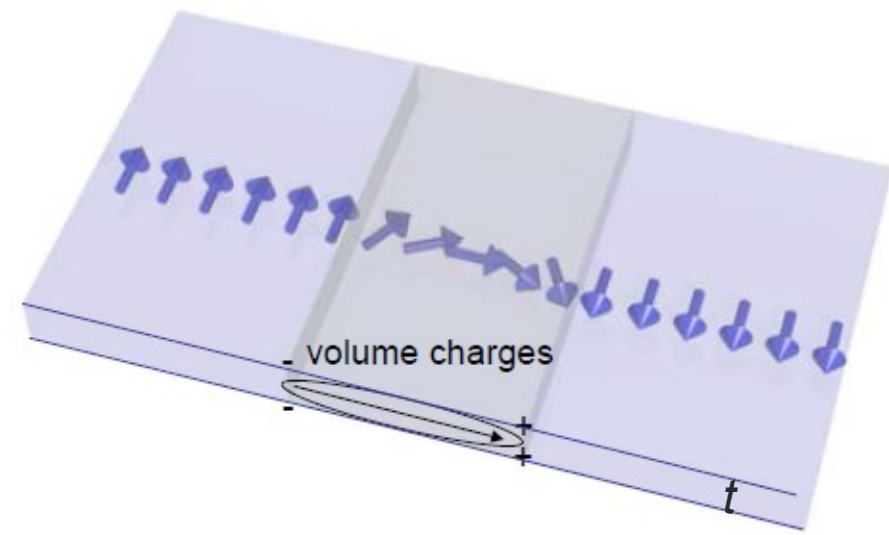
- Néel and Bloch domain walls for in-plane magnetized systems

Bloch wall



Domain wall width $d_w < t$

Néel wall

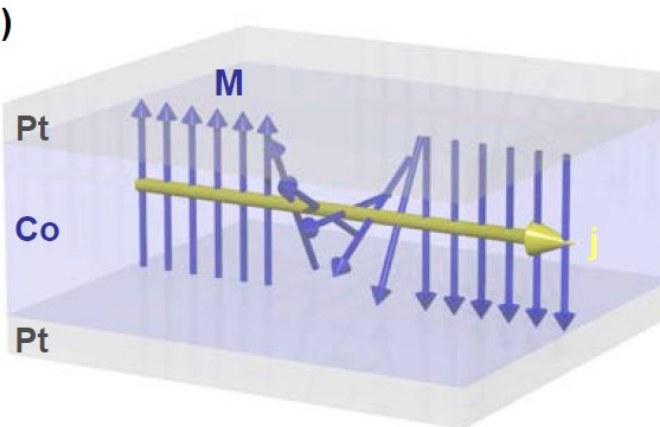


Domain wall width $d_w > t$

Ferromagnetism in a nutshell – Domains and Walls

- > Néel and Bloch domain walls for films with perpendicular anisotropy

Bloch wall



Néel wall

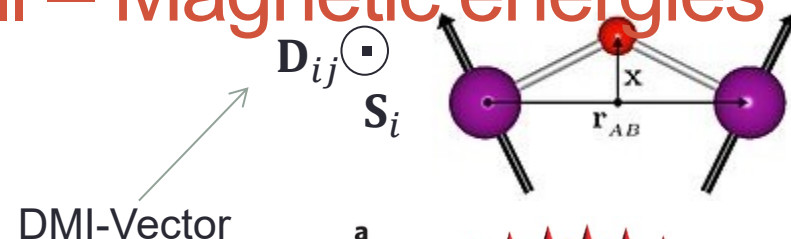
- No magnetic charges in wall!

- exhibits volume charges (unfavorable due to magnetostatic energy)
but
- Néel wall favored by Dzyaloshinskii-Moriya interaction (considered since 2013!)

Ferromagnetism in a nutshell – Magnetic energies

- Dzyaloshinskii-Moriya interaction (DMI):
Asymmetric exchange interaction

$$E_{\text{DMI}} = \sum_{i \neq j} \mathbf{D}_{ij} (\mathbf{S}_i \times \mathbf{S}_j)$$



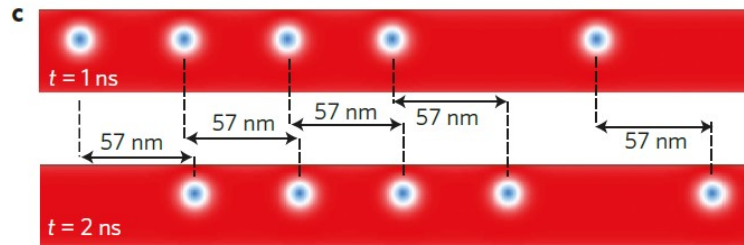
→ Minimization of total energy yields to formation of chiral structures = 'skyrmions'

- Asymmetric magnetic multilayers like Pt/Co/Ir**

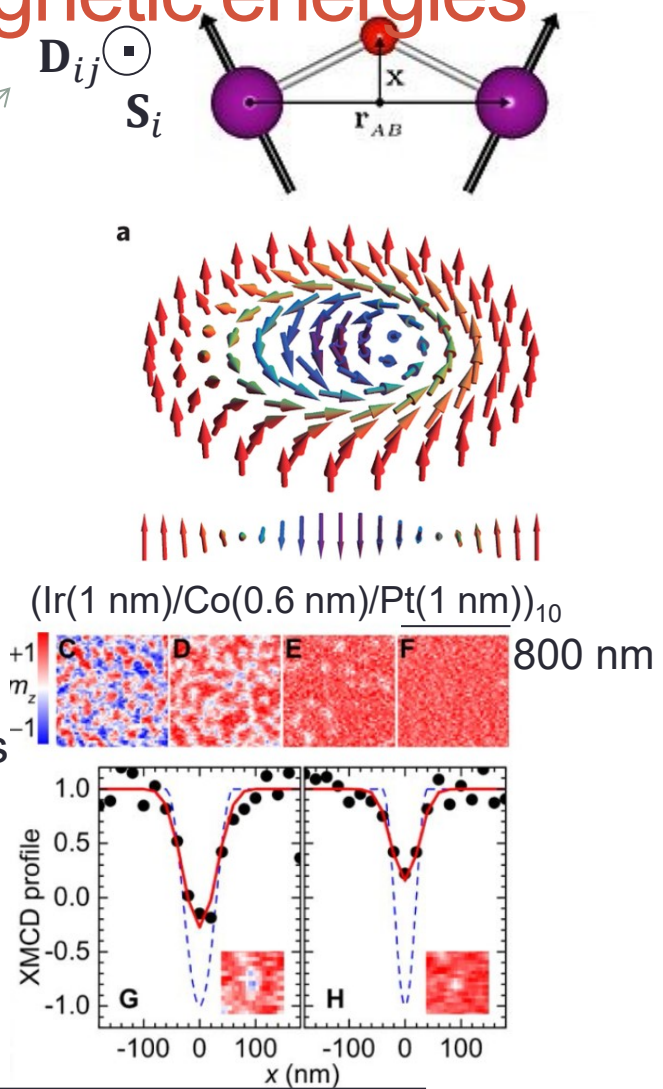
Different sign of \mathbf{D}_{ij} for Co/Pt and Co/Ir interface

→ additive, large effective DMI

- Future Skyrmion-based memory & data storage devices



J. Sampaio, A. Fert et al., Nat. Nanotech. 8, 839 (2013)

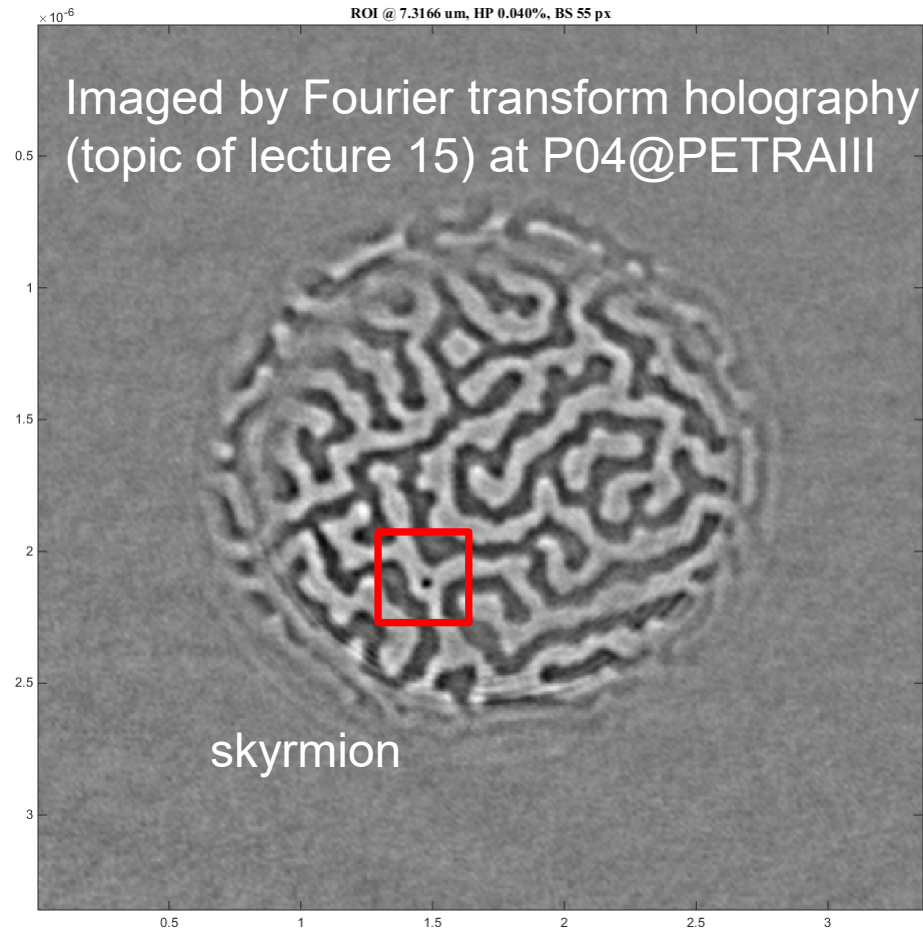
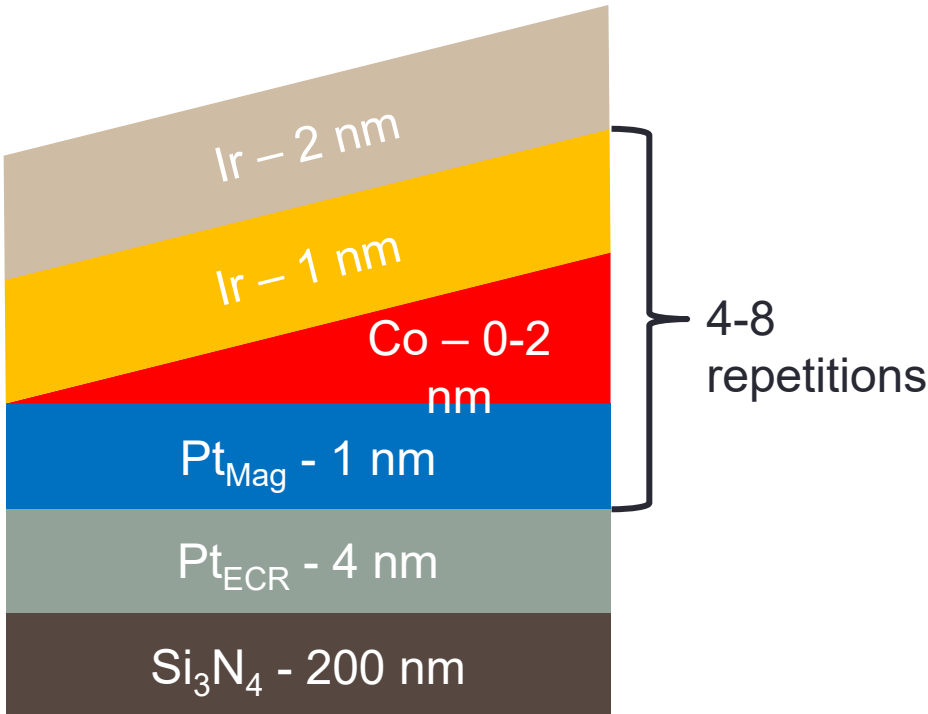


C. Moreau-Luchaire, A. Fert et al., arXiv:1502.07853v1 (2015)

Ferromagnetism in a nutshell – Domains and Walls

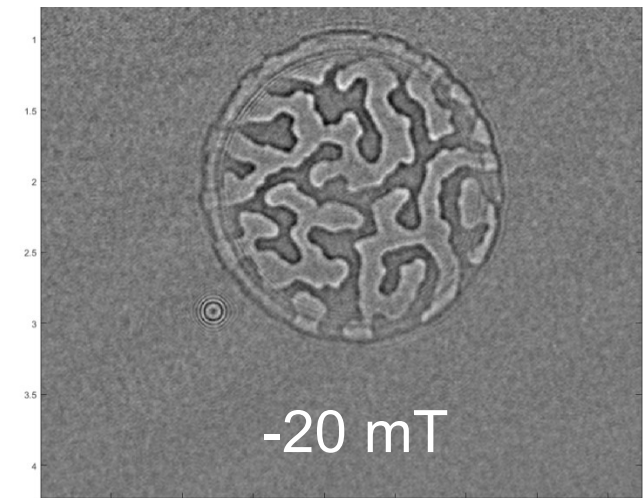
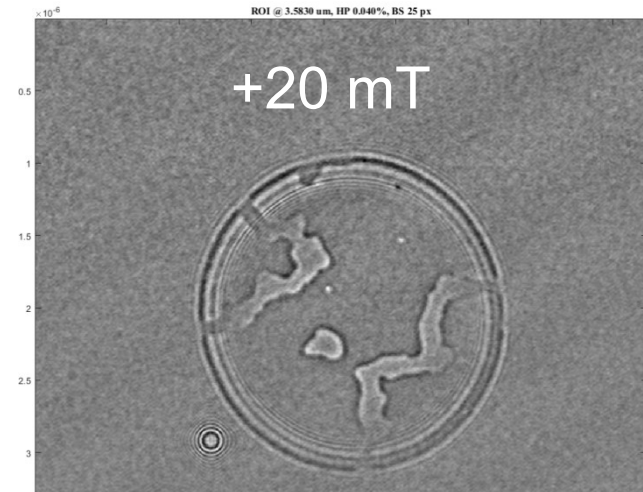
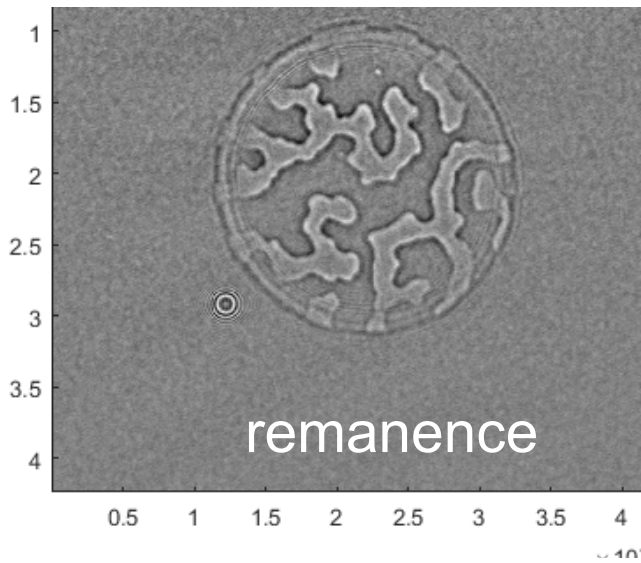
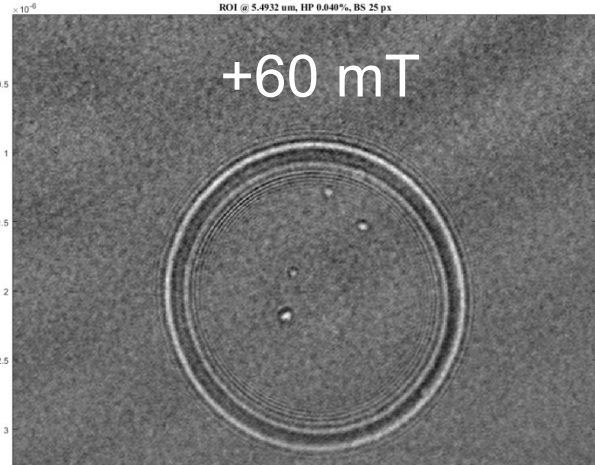
- What we are doing?

Pt/Co/Ir Multilayers



Ferromagnetism in a nutshell – Domains and Walls

- Out-of-plane field sweep



Ferromagnetism in a nutshell – Domains and Walls

- Current induced Skyrmiion motion

